AN UNDER-ACTUATED MECHANISM FOR AN ANTHROPOMORPHIC PROSTHETIC HAND

Rajapakse Pathirage Don Denuwan Chamara

(168656J)

Thesis/Dissertation submitted in partial fulfillment of the requirements for the degree Master of Science

Department of Electrical Engineering

University of Moratuwa

Sri Lanka

February 2020

DECLARATION

I declare that this is my work and this thesis does not incorporate without acknowledgement any material previously submitted for a Degree or Diploma in any other University or institute of higher learning. To the best of my knowledge and belief, it does not contain any material previously published or written by another person except where the acknowledgement made in the text.

Also, I hereby grant to the University of Moratuwa the non-exclusive right to reproduce and distribute my thesis/dissertation, in whole or in part in print, electronic or other media. I retain the right to use this content in whole or part in future works (such as articles or books).

Signature: Date:

The above candidate has researched for the Master's Thesis under my supervision

Name of the supervisor Prof. Ruwan Gopura

Signature of the Supervisor Date:

ABSTRACT

Upper limbs are very important to the functionality of the human body that enables us to execute activities of daily life (ADL). The human upper limb is complex and difficult to mimic from a robotic manipulator. Over the years the evolution of robotic prosthetic hand development is evident, which brings robotic prosthetic hands closer to the human hand performance. The challenge is to develop a robotic prosthesis with fewer actuators, human-like appearance and convenient interaction for the amputee. This research focuses on developing an under-actuated mechanism for a robotic prosthetic hand while maintaining the anthropometry of the human hand. This under-actuated mechanism primarily generate three grip patterns, namely index finger extended, pinch grip, and power grip. The under-actuated mechanism consists of a clutch mechanism that uses two actuators for controlling flexion and extension of fingers excluding thumb. This reduces control hardware whilst enabling to build a functional under-actuated mechanism incorporating 3D printing for creating lightweight prosthesis. Initial CAD models enabled to check the feasibility of under-actuated robotic hand design and various simulations helped to verify the design. For developed prosthesis hand, the mathematical kinematic model was constructed which was fed into the Matlab software to evaluate effectiveness of motion generation of fingers.

DEDICATION

To the most courageous three individuals who guided me to great achievements: My beloved Father Ajith Premalal, Mother Indrani Jayasekara and Sister Dulanjalee Sachittra.

ACKNOWLEDGMENT

As a graduate student at the Faculty of Engineering, University of Moratuwa, I have to complete a Research Project for the partial fulfillment of the requirements for the MEng/PG Diploma in Industrial Automation. For that, I selected the topic “An Under-actuated Mechanism for Anthropomorphic Robotic Prosthetic Hand”. I am highly indebted to the University of Moratuwa for their guidance and constant supervision as well as for providing necessary information regarding the project and for their support in completing the special studies project. I would like to express my gratitude towards Prof. Ruwan Gopura for his kind cooperation and encouragement that helped me in the completion of this project. He has always guided me with immense generosity. Further, I acknowledge Dr. Buddika Jayasekara for his valuable comments on my research and guiding me in the correct direction to be successful in achieving the final goal. My thanks and appreciations go to my colleagues in developing the project and people who have willingly helped me out with their abilities.

R.P.D.Denuwan Chamara

TABLE OF CONTENTS

LIST OF FIGURES

LIST OF TABLES

CHAPTER 01 : INTRODUCTION

Loss of human limbs occurs due to various reasons such as congenital diseases, accidents, illness or birth defects. This ultimately results in the disruption of activities of daily life for the amputee. From the early years, humans have always looked at developing these apparatus know as prosthesis (artificial wearable limb) replaces a missing extremity [1].

Congenital deformity, tumors, traumatic accidents and vascular complications due to diabetes or other diseases are to be the most frequent causes for upper-limb amputation [2]. Statistical data shows that around 60 % of the total wrist and hand amputation are trans-radial (below-elbow) amputations [2]. Hence, it is crucial for research and development of a cost-effective and simplistic design for trans-radial prosthetic devices. Over the years of research and development of human prosthesis, it is hard to mimic human performance. Although contemporary trans-radial prosthesis show deficiencies in restoring the actual performance of biological wrist and hand, prominent improvements in functionality, versatility, and control are noted over predecessors [3]. However, amongst all technological developments of prosthetic hand, most amputees do not use a prosthesis to support activities of daily life (ADL) due to various reasons [4]. This clearly shows that there is room for further research and development to deliver prosthesis that feels like a natural extension of the human body.

Functional commercial prosthesis available in the current market is costly and developing countries such as Sri Lanka cannot benefit. Hence, Search for functional yet cost-effective solutions are essential, which is what this research focuses on. One way to tackle this problem is to reduce the degrees of freedom of the prosthetic hand, but this will affect the complexity and versatility of the prosthetic hand. Another approach is lowering the number of actuators without decreasing the degrees of freedom. In other words, fewer actuators than degrees of freedom are included in the design [5]. This concept commonly referred to as under-actuation that incorporates passive components such as springs and mechanical modules such as clutches.

Development of human-like (anthropomorphic) prosthesis is a controversial topic. Literature shows that trans-radial amputees are demotivated to wear prostheses that do not have a human hand appearance. It is important to have anthropometric features in prosthetic hands since humans use a range of gestures for communication purposes. Therefore, many researchers [6], [7] look upon researches on anthropomorphic designs. With the recent

advances in humanoid robotics, there is a strong need for anthropomorphic hands that are light, compact, easy to control and versatile enough to grasp a broad variety of objects. Considering the current state of the art actuator and sensor technology, under-actuation is one of the most promising avenues for the development of anthropomorphic hands.

In recent years, communities and startups of open source projects use of 3D printing in prosthetics. This is mainly because prosthetics require a highly individualized and flexible approach that involves low cost [8]. Advance sensors with intelligent control algorithms are present to capture amputee signals for operating functional prostheses. EMG (electromyography) sensors for detecting muscle flex and IMU (Inertial measurement unit) sensors for detecting rotations control the prosthesis. Algorithms enable the amputee to feed different grasp patterns into a prosthetic hand. Development in the field of the prosthesis in the past few decades in Sri Lanka had been slow in comparison with neighboring Asian countries [9]. With increasing population, aging and human disabilities, the field of prosthetics and orthotics continuously researched. Improved orthopedic services will demand more access to prosthetics and orthotics. Hence, concentrated effort by all stakeholders with current technological advancements to cater to the quality of prosthesis and orthotics services and increase the benefits of such services.

1.1 Contribution of the thesis

The research work presented in this thesis is towards the development of an under-actuated mechanism for an anthropomorphic robotic prosthetic hand. Below outlines the major contributions.

- Developed an anthropomorphic trans-radial prosthetic hand
- Developed a novel under-actuated clutch mechanism for finger actuation
- Carried out kinematic analysis of under-actuated mechanism

1.2 Thesis overview

The thesis consists of four chapters. The organization of the thesis is as follows. Chapter 2 covers the literature review. Chapter 3 explains the prosthesis and design comprehensively. Chapter 4 describes the control circuit in depth. Chapter 5 proposes the simulation and experiments and finally, chapter 6 concludes the thesis with further direction.

Chapter 2 – Literature review

This chapter covers the biomechanics of the human hand and currently available prosthetic controllers commercially and at the research level. Discussion of how biomechanics plays a vital role in designing robotic anthropomorphic prosthetic devices. Includes literatures relevant to the under-actuated mechanism was reviewed in this chapter along with the evolution of prosthetic controllers.

Chapter 3 – Proposed prosthetic hand design

This chapter covers the design aspects of the proposed under-actuated prosthetic hand. Discussions of the design of fingers with mathematical model using the kinematic analysis are included. The internal working and design methodology used to develop the under-actuated clutch module was reviewed extensively. Finally, this chapter also covers prosthetic hand operational flow and fabrication procedure of components.

Chapter 4 - Control system

This chapter primarily discusses the control hardware and control algorithm. In detail review of specifications and applications of hardware components used in the development of prosthetic hand. The defined control algorithm used in prosthetic device along with test setup used to control developed prosthetic hand.

Chapter 5 – Simulation and experiments

This chapter covers simulation concerning motion analysis of prosthetic hand operation. Displacement of the cam profile was also evaluated using software discussed under this chapter. Includes experimental results compared with the expected outcome along with justification and achievement of research.

Chapter 6 – Conclusion

This chapter concludes the thesis with future directions

CHAPTER 02 : LITERATURE REVIEW

Figure 2.1 Civil war prosthesis hook

Since the beginning of the time history of the prosthesis is exciting and evolving, humans have understood the need to replace lost limbs for functional, cosmetic and spiritual reasons. We can observe from ancient civilizations of Egypt, Greece, and Rome who have pioneered the development of science and medicine that led to the development of first prosthetics. World War I and II, which caused loss of work force in the USA and Europe, triggered recent prosthesis developments. Figure 2.1 that illustrates civil war prosthesis hook. Integrating technology with prosthesis to create smart prosthesis was in the concept of Cybernetics in 1948, the study of control and communication between human and machine played a significant role later on for the improvement of the prostheses [10]. In 1949, first electrically operated arm prosthesis developed in the United States by the state government and IBM Corporation led by Samuel Anderson [11]. Initially, Russians used myoelectric sensors in prosthesis hands in 1958. Ottobock Company made this prosthesis commercially available for the public [11]. Over the years, researchers have undertaken this daunting task of developing prostheses to mimic human limbs or sometimes to be better than human limbs itself. However, most high end advanced functional prosthesis is expensive and developing countries like Sri Lanka cannot afford. Hence, more research towards developing cost-effective prostheses integrating the latest technology and innovative ideas should be encouraged. However, the tradeoffs between functionality, reliability, affordability and appearance are not fully settled.

2.1 Human hand anatomy

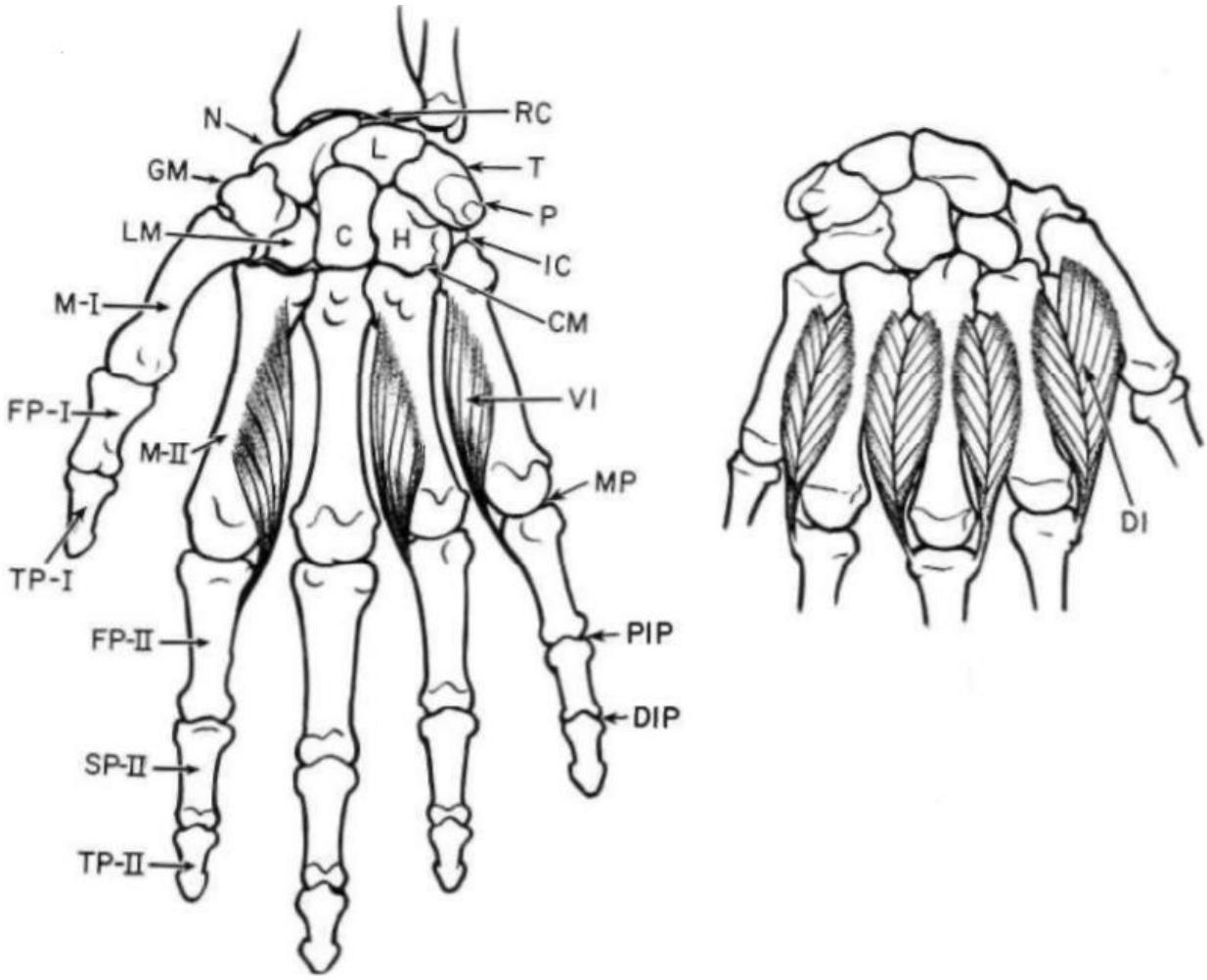

(a) **(b)**

Figure 2.2 Bones and articulations of the hand, (a) - volar view; (b) - dorsal view [12]

It is obvious to all that the human hand represents a mechanism of the most intricate fashion and one of great complexity. In any mechanism, animate or inanimate, functional capabilities relate to both structural characteristics and the nature of the control system available for management of functions singly or in multiple combinations. Just so, with the human hand analysis characteristics, therefore, require an understanding of both sensory and mechanical features [12]. The bones of the hand, shown in Figure 2.2, naturally group themselves into the carpus, comprising eight bones that make up the wrist and the root of the hand, and the digits, each composed of its metacarpal and phalangeal segments (Table 2.1).

Table 2.1 Bones and Joints of the hand and the wrist with reference to Figure 2.2

Carpel bones	
GM	Greater multangular
N	Navicular
L	Lunate
T	Triquetrum
P	Pisiform
LM	Lesser multangular
C	Capitate
H	Hamate
Metacarpal bones	
M-I, II, III, IV, V	
First phalangeal series	
FP-I, II, III, IV	
Second phalangeal series	
SP-II, III, IV, V	
Third phalangeal series	
TP-I, II, III, IV, V	
Joints	
RC	Radiocarpal
IC	Intercarpal
CM	Carpometacarpal
MP	Metacarpophalangeal
PIP	Proximal interphalangeal
DIP	Distal interphalangeal

2.1.1 Human hand bone structure

The carpal bones arranged in two rows, those in the more proximal row articulating with radius and ulna. Between the two are the inter-carpal articulations. The bony conformation and ligamentous attachments are such as to prevent both lateral and dorsal-volar translations, but to allow participation in the major wrist motions as shown in Figure 2.3. In each of the digits, the anatomical design is essentially the same, with exceptions in the thumb. Metacarpals II through V articulate so closely with the adjacent carpal bones of the distal row that, although they are capable of some flexion and extension, independence of motion is very limited. The metacarpal shafts arched to form the palm, and the distal ends are almost hemispherical to receive the concave curvature of the proximal ends of the first phalanges. The meta-carpo-phalangeal joint exhibits a pattern seen also in the inter-phalangeal joints. The virtual center of rotation lies approximately at the center of curvature of the distal end of the proximal member.

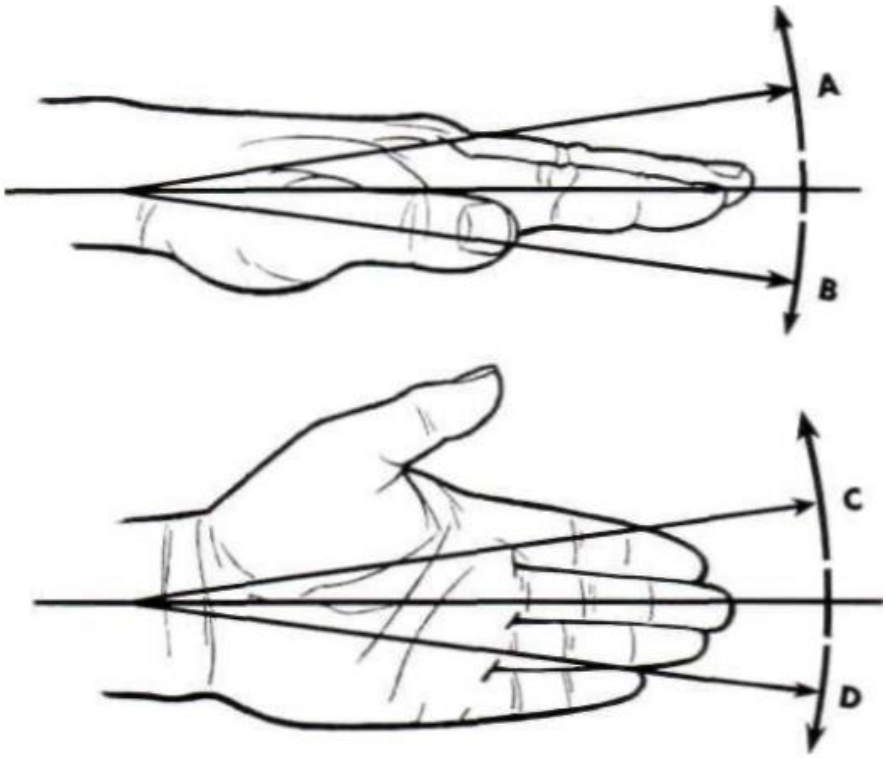

Figure 2.3 Angles of rotation about the wrist, A: extension (or dorsiflexion); B: flexion (or volar flexion); C: radial flexion; D: ulnar flexion [12]

The lateral aspects of the joint surfaces narrowed and closely bound by ligaments, so that lateral rotation is small in the meta-carpo-phalangeal joints and lacking entirely in the phalangeal articulations. Hence, the latter is typical hinge joints. The thumb differs from the other digits first in that the second phalanx is missing and, second, in that there is greater mobility in the carpometacarpal articulation. For conceptual development of prosthesis hand proposed in this study, studying human hand joints is critical. When we look into a finger, there are four joints in each finger, in sequence, from the proximal to distal, which are carpometacarpal (CMC), meta-carpo-phalangeal (MCP), proximal inter-phalangeal (PIP), and distal inter-phalangeal (DIP) joints. The CMC joints formed by the bases of the four metacarpals and the distal carpal bones and are stabilized by interosseous ligaments to form a relatively immobile joint. However, a major function of the CMC joint is to form the hollow of the palm and allow the hand and digits conform to the shape of the object being handled [13] [14]. The MCP joints are composed of the convex metacarpal head and the concave base of the proximal phalanx and stabilized by a joint capsule and ligaments. The range of flexion differs among fingers with the index finger having the smallest flexion angle of 70 degrees and the little finger showing the largest angle of 95 degrees [14] [15]. Radial and ulnar deviation of approximately 40 to 60 degrees occur in the frontal plane, with the index finger

showing up to 60-degree abduction and adduction, the middle and ring fingers up to 45 degrees, and the little finger about 50 degrees of mostly abduction[16]. The range of motion of the MCP joint decreases as the flexion angle increases because of the bicondylar metacarpal structure [17] [14]. There is also some axial rotation of the fingers from a pronated to a supinated position as the fingers extend. In the reverse motion, the fingers crowd together as they enter flexion [16] [14]. The IP joints, as hinge joints, exhibit only flexion and extension. Each finger has two IP joints, the PIP and the DIP, except the thumb, which has only one. Volar and collateral ligaments, connected with expansion sheets of the extensor tendons, prevent any side-to-side motion. In the PIP joints, the largest flexion range of 100 degrees to 110 degrees is present. While a smaller flexion range of 60 degrees to 70 degrees found in the DIP joints. Hyperextension or extension beyond the neutral position, due to ligament laxity, also be found in both DIP and PIP joints [16] [14].

2.1.1 Human hand muscle structure

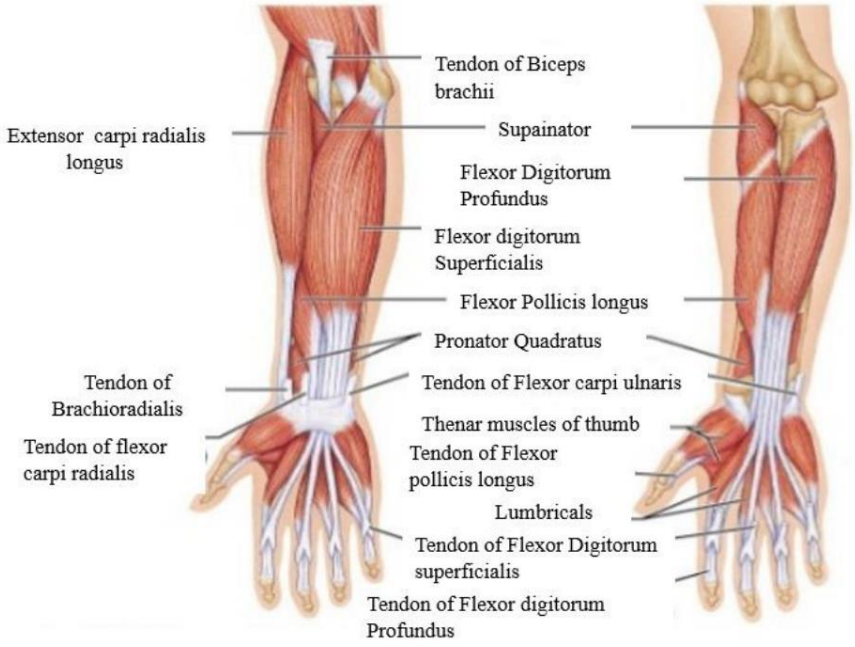

Figure 2.4 Anterior muscles of the right hand [18]

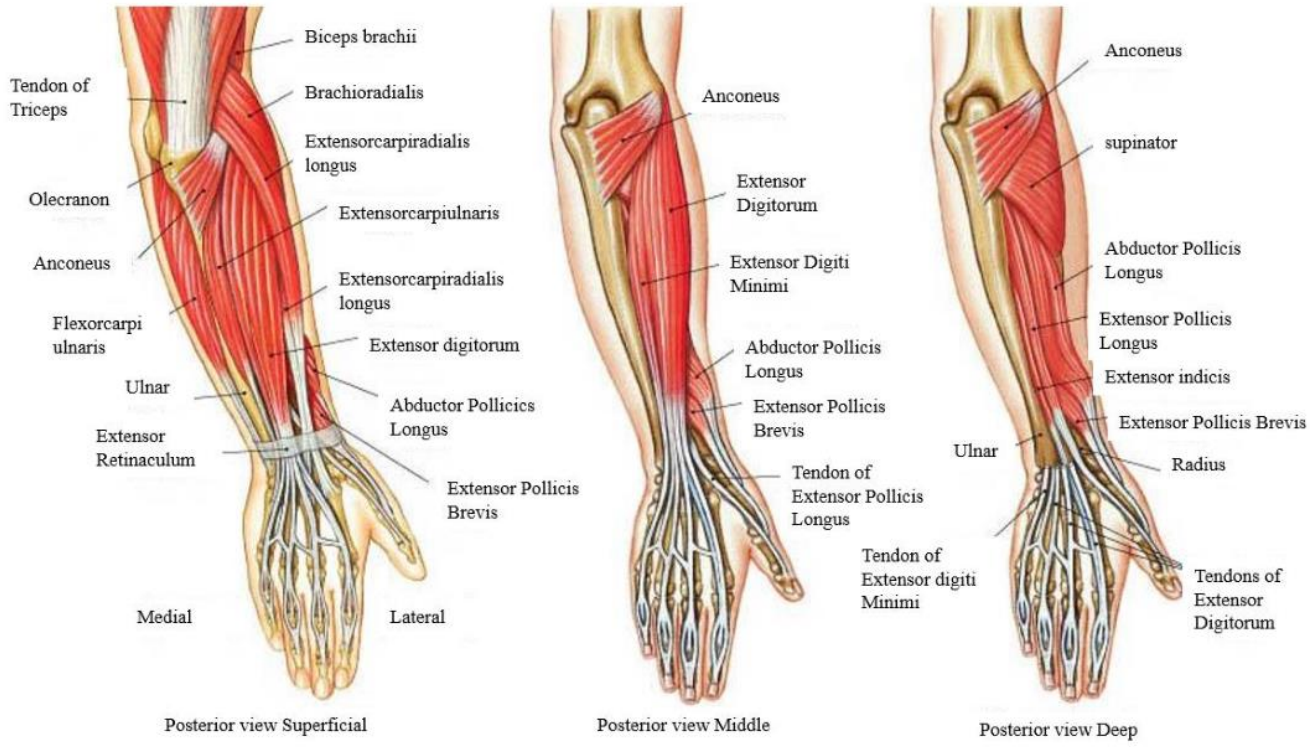

Figure 2.5 Posterior muscles of the right hand [18]

Table 2.2 Extrinsic Muscles of hand and wrist [14]

Group	Layer	Name	Nerve	Function
Anterior	Superficial	Flexor carpi radialis	Median	Flexes and adducts hand, aids in flexion / pronation of forearm
		Palmaris longus	Median	Flexes hand
		Flexor carpi ulnaris	Ulnar	Flexes hand adducts hand
	Middle	Flexor digitorum superficailis	Median	Flexes phalanges and hand
	Deep	Flexor digitorum profundus	Median, Ulnar	Flexes phalanges and hand
Posterior	Superficial	Extensor carpi radialis longus	Radial	Extends and abducts hand
		Extensor carpi radialis brevis	Radial	Extends hand
		Extensor digitorum	Radial	Extends little finger
		Extensor digiti minimi	Radial	Extends little finger
		Extensor carpi ulnaris	Radial	Extends and adducts hand
	Deep	Abductor pollicis longus	Radial	Abducts thumb and hand
		Extensor pollicis brevis	Radial	Extends thumb
		Extensor pollicis longus	Radial	Extends thumb
		Extensor indicis	Radial	Extends index finger

Figure 2.4 and 2.5 show anterior and posterior of the right hand respectively, and Table 2.2 elaborates on extrinsic muscles of hand and wrist. The muscles moving the finger are in two groups extrinsic and intrinsic based on the origin of the muscles. The extrinsic muscles originate primarily in the forearm, while the intrinsic muscles originate primarily in the hand. Therefore, the extrinsic muscles are large, provide strength, while the intrinsic muscles are small, and provide precise coordination of the fingers. Each finger innervated by both sets of muscles, requiring good coordination for hand movement [14]. The flexor digitorum profundus (FDP) and flexor digitorum superficialis (FDS) is the main finger flexor muscles and are involved in the most repetitive work.

2.2 Types of prosthesis

There are six basic prosthetic options to consider for the upper extremity amputee. The type of prosthesis needed depends on the level of amputation, the condition of the residual limb, individual goals and work requirements, and other variables. An individual often needs more than one prosthetic device to accomplish all of his or her goals. Personal requirements may be function-related, cosmetic or psychological [19].

2.2.1. Electrically-powered prosthesis

This category of prosthesis uses small electric motors in the terminal device (hand or hook), wrist and elbow. A rechargeable battery system powers the motors and electric motors operate the hand function, its grip force is significantly increased [19].

2.2.2. Cosmetic restoration

Cosmetic restoration, or duplication of the contralateral arm or hand, is a popular prosthetic option. This involves replacing what was lost from amputation or congenital deficiency with prosthesis similar in appearance to the non-affected arm or hand and provides simple aid in balancing and carrying [19].

2.2.3. No prosthesis

Not all people are candidates for a prosthesis, and even if they are, many choose not to wear one. Only half of all upper extremity amputees ever receive prosthetic services. Half will stop using their prosthesis during the first year. For many amputees, use of the prosthesis does not satisfy their level of function. Others, without adequate funding, may receive a prosthesis that does not address their individual needs or that cause pain and discomfort and they discontinue further prosthetic care [19].

2.2.4. Body-powered prosthesis

Body-powered (or conventional) prosthesis use gross body movements of the shoulder, upper arm, chest, etc. Harness system attached to a cable and connected to a terminal device (hook) or hand captures the movements. Some levels of amputation or deficiency allow an elbow system for improved function [19].

2.2.5. Activity-specific prosthesis

Design of an activity-specific prosthesis is for an activity that requires some function or durability that other prostheses cannot provide. Often created for recreational activities such as fishing, swimming, golfing, hunting, bicycle riding and weight lifting, for music or work-related tasks have also been designed [19].

2.2.6. Hybrid prosthesis

Hybrid prosthesis combines body power and electrical power. Most hybrid prostheses for individuals with trans-humeral (above the elbow) amputations or deficiencies are used [19].

2.3 State of the art robotic prosthesis

Many research improvements over functional prostheses are present, which challenge recent researchers to design and build versatile robotic prosthetic hands. Some of pioneering robotic prosthetic hands include Bebionic hand [20], UTAH hand of MIT [21], Stanford hand of JPL [22], Belgrade hand of USC [23], DLR hand [24], iLimb hand of touch bionics [25] and Vincent hand [26]. Apart from these prosthetic hands, many researches exist for finding an optimal design between versatility and simplicity to achieve suitable practical systems for amputees. In order for the amputee to feel natural motion generation, the prosthesis should have the features of natural human hand, especially anthropometric features. It is important to have anthropometric features in prosthetic hands since humans use hands for several daily activities and a range of gestures for communication purposes. Therefore, many researchers [6] look upon researches on anthropomorphic designs, [7]. Control methodologies scrutinized on how well they respond to the motion, intention of the wearer. The most notable development is the myoelectric arm. It uses surface electromyography signals from the muscles of the residual limb or shoulder to derive predefined patterns of finger movements. With the aid of the rigorous training process, proportional movements are possible.

Table 2.3 Categorized general characteristic of modern prosthesis hands

Name	Sensors	country of origin	Weight (grams)	DoF	No. of actuator	Finger movement mechanism	Actuation method
MANUS Hand [28]	Force and position sensors	USA	850	7	2	Tendon based mechanism and crossed bar mechanism	Brushless DC motors
LUCS Haptic Hand III [29]	Tactile sensors	Sweden	700	12	6	Tendon based mechanism	RC servo motors
DLR/HIT II Hand [30]	position, force/torque and temperature sensors	Germany/ China	1500	15	15	Belt drivers and gears based mechanism	Brushless DC motors with harmonic drive
Keio Hand [31]	No sensors	Japan	853	20	20	Wire driving method using elastic elements	Ultrasonic motor
Fluid Hand III [32]	Force sensor	Germany	400	8	5	Flexible fluidic actuators	Pressurized fluid
Vanderbilt Multigrasp Hand [33]	No sensors	USA	750	9	4	Tendon and torsion spring based mechanism	Brushless DC servo motors
Smart Hand [34]	Tactile, tension sensor and limit switch	Italy	530	16	4	Tendon and torsion spring based mechanism	DC motors with using worm gears
UNB Hand [35]	Force and slip sensors	Canada	746	5	3	Linkage based mechanism	DC motors
DEKA RC Gen3 arm [36]	Position and tactile sensor	USA	4445	6	4	Linkage based mechanism	Both brushless and brushed DC motors
U Grip II [37]	Force sensors	USA	600	5	5	Pneumatic artificial muscles (PAMs)	pneumatic
UOM Transradial prosthesis [1]	No sensors	Sri Lanka	500	7	3	Cross-bar mechanism	Brushless DC motors with gear drives

The emphasis is on development of wearable sensors to control the prostheses more precisely [27]. Most of the trans-radial prostheses are developed to perform specific tasks, where the controlling is limited to one or few operations and generally not smooth in functioning compared to the natural hand [38]. Due to the strict limitations on prosthetic device size, shape and weight, the performance and functionalities have to be traded-off. Throughout this paper, research-level prosthetic devices benchmark the performance, compare various mechanical designs, and control methodologies. Table 2.3 shows the categorization of well-known prosthetic devices among various parameters. In the design and development of trans-radial prosthesis, the key factors are size, shape, weight, durability, appearance and functional capabilities. Besides, there is a need for establishing a proper scheme for evaluating the available prosthetic devices employing user acceptance, anthropometry, and ergonomics, functional capabilities, etc. Considering the current developments, modern trans-radial prostheses are moving closer to a state where they can mimic the biological wrist and hand. However, their availability to the general amputee population is as large unsatisfactory due to the extreme costs involved. This necessitates further innovation in the design of hardware and control systems for trans-radial prostheses.

CHAPTER 03 : PROPOSED PROSTHETIC HAND

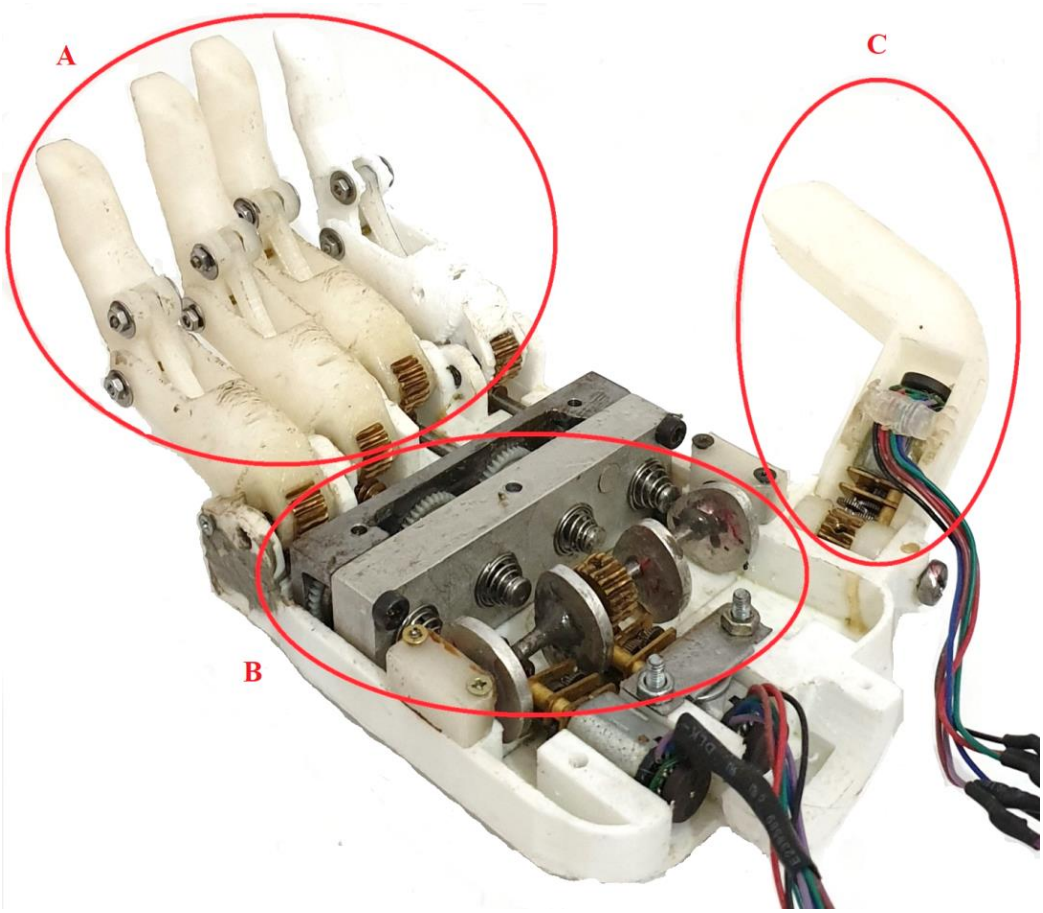

Figure 3.1 Developed prototype prosthetic hand with three main modules

The development of an under-actuated mechanism for an anthropomorphic robotic prosthetic hand started with an initial feasibility study. Study of various types of clutch mechanisms, under-actuated mechanism and subject related literature helped to gather knowledge. CAD models were developed and simulated for under-actuated mechanisms that ensured prototypes built will not result in any problems. However, some prototypes failed in actual operation that led to better development of the final prototype. Figure 3.1 depicts three main components that make up the proposed prosthetic hand, namely A- Finger unit, B- Clutch unit and C- Thumb unit. These three components were designed modular wise for convenient development. Design and development along with working principal in detailed review of these three components are present in future chapters.

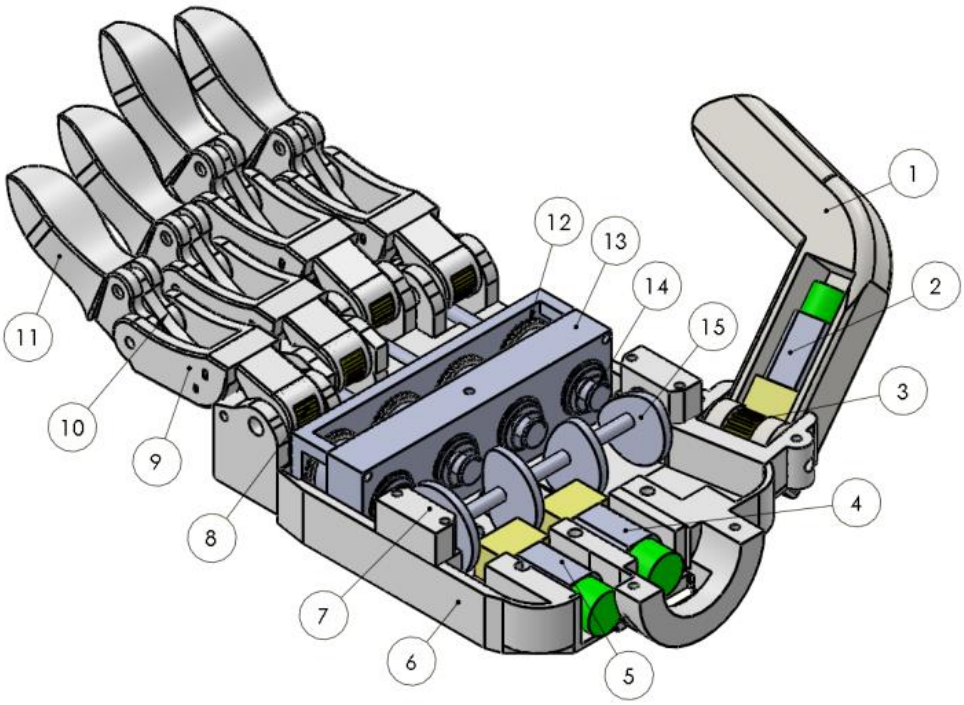

Figure 3.2 3D model developed for under-actuated prosthetic hand

Table 3.1 Components of prosthetic hand with reference to Figure 3.2

Part no	Part Name	Function
1	Thumb housing	Thumb structure houses the motor and gear wheels for actuating thumb flexion and extension.
2	DC gear motor with encoder	This motor actuates thumb flexion and extension movement and tracks thumb position with built-in encoder feedback.
3	Worm gears	Worm rod and wheel create motion transmission from motor to thumb housing for movement.
4	DC gear motor with encoder	This motor actuates camshaft via worm gear and keeps track of camshaft position using an encoder.
5	DC gear motor with encoder	This motor drives motion into a clutch module and keeps track of clutch motion.
6	Palm bottom housing	Houses main components
7	Camshaft bearing housing	Houses bearing for smooth motion of CAM-shaft.
8	Worm gears	Transmits motion into fingers from clutch module
9	Proximal phalange	Component mimicking mid-section of human finger
10	Link	Connects distil finger to palm bottom housing.
11	Distal phalange	Mimics human distal phalange and aids in griping objects
12	Clutch module drive gears	Transmits rotational motion from motor to clutch module
13	Clutch module housing	Houses clutch components such as gears, clutch female and male plates.
14	Clutch engage pins	Cam comes in contact with this pin which in turn activates the clutch
15	Camshaft	Camshaft rotates to engage the clutch and in turn actuates fingers according to the clutch pattern.

Figure 3.2 shows the final developed 3D model of an under-actuated anthropomorphic robotic prosthetic hand. This design incorporates a novelty under-actuated mechanism that is the key component of this design. The under-actuated mechanism consists of a camshaft that is responsible for clutch engagement and actuating fingers for motion. The camshaft is responsible for the sequence of finger selection. Two DC gear motors with inbuilt encoders, drive the camshaft and clutch drive mechanism. Actuation of thumb occurs with an independent worm gear and dedicated DC gear motor with inbuilt encoder. In detail, the description of the finger design and the under-actuated mechanism in further chapters with operating principals of the developmental hand are present. Table 3.1 provides the details of important components that make up the under-actuated prosthetic hand regarding Figure 3.2. Appendix A shows the complete outline drawing of the final assembly hand.

3.1 Design of fingers

Four bar mechanism is present in all fingers excluding the thumb. This mechanism, specifically crossed four bar mechanism is responsible for mimicking human finger flexion and extension. Distal phalange consists of a fixed angle that eliminates the need for additional linkages. In this arrangement, proximal phalange would rotate and follow the four-bar mechanism. Output shaft of the clutch module links with MCP joint using worm gears. Mechanical links couple the MCP, PIP and DIP joints. Since the crossed four-bar linkage mechanism consists of one degree of freedom, the proposed design also consists of one degree of freedom for each finger. Hence, a total of 5 degrees of freedom for the entire robotic prosthesis hand. Figure 3.3 shows the four-bar mechanism in a finger mechanism alongside actual developed finger. Using mobility formulae – Kurtzbach equation degree of freedom of a single finger deduced as follows:-

$$F = 3\left(L - 1\right) - 2(J) - h\,(x) \tag{3.1}$$

In (3.1) where; F = total degrees of freedom in the mechanism

L = number of links (including the frame)

J = number of lower pairs (one degree of freedom)

h = number of higher pairs (two degrees of freedom)

$$F = 3\,(\,4 - 1) - 2(4) - 0$$

$$F = 1$$

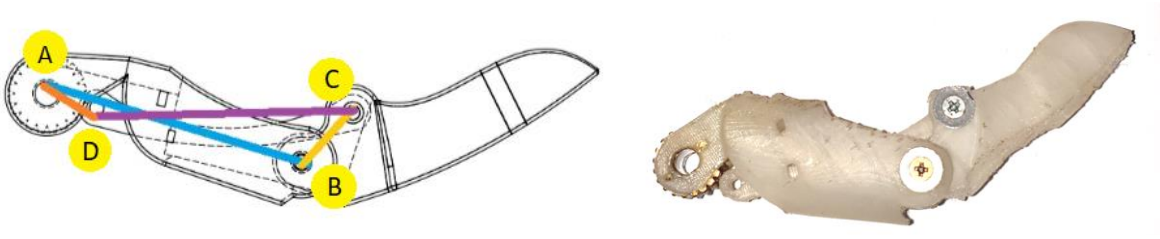

(a) **(b)**

Figure 3.3 (a) 3D model and (b) actual prototype developed for under-actuated prosthetic hand

3.2 Kinematic analysis of finger

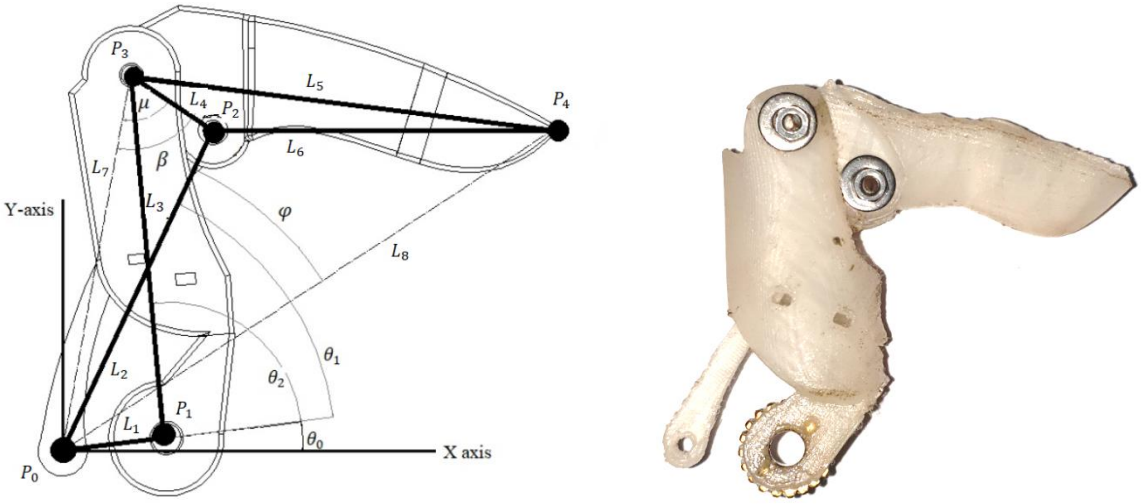

(a) **(b)**

Figure 3.4 (a) Kinematic model with labeled variables and (b) actual snapshot of finger for comparison

A developed kinematic model for prosthetic finger enabled to calculate finger operation scope. Further study of kinematic model and analysis of linkages and joints in motion was possible with Matlab software. Kinematic diagram of the mechanism as shown in Figure 3.4; points P_0, P_1, P_2, and P_3 are considered as a crossed four-bar mechanism. The relationship between links satisfies the double-crank inversion defined by the Grashoff condition. Angles of a triangle made with points P_2, P_3 and P_4 remain constant as this triangle acts as the coupler triangle. As shown in Figure 3.4 link length L_1, L_2, L_3, and L_4 are 9 mm, 36 mm, 37 mm and 10 mm respectively. Additionally, L_5 and L_6 link lengths are 43mm and 34 mm respectively.

Consider points P_0, P_1, P_2, and P_3 as a crossed four-bar mechanism. Each point's position was calculated about P_0. Angle θ_1 serves as the reference angle for which values of other angles are based upon.

$$L_4{}^2 = (L_2 \cos\theta_1 - (L_1 + L_3 \cos\theta_2))^2 - (L_2 \sin\theta_1 - L_3 \sin\theta_2)^2 \quad (3.2)$$

(3.2) could be re-arranged as follows;

$$L_4{}^2 - L_2{}^2 - L_3{}^2 - L_1{}^2 + (2)(L_1)(L_2)\cos\theta_1 = (2)(L_3)\cos\theta_2\,(L_1 - L_2\cos\theta_1) + (-(2)(L_2)\,(L_3)\sin\theta_1)\sin\theta_2 \quad (3.3)$$

(3.3) could be reduced to Freudenstein equation and written as follows;

$$K_1 = K_2 \cos\theta_2 + K_3 \sin\theta_2 \quad (3.4)$$

In which;

$$K_1 = \frac{L_4{}^2 - L_2{}^2 - L_3{}^2 - L_1{}^2 + (2)\,(L_1)(L_2)\cos\theta_1}{2(L3)}$$

$$K_2 = L_1 - L_2 \cos\theta_1$$

$$K_3 = -L_2 \sin\theta_1$$

(3.4) solved using half-angle tangent trigonometric identities;

$$K_1 = \left(\frac{1 - \left(\tan\frac{\theta_2}{2}\right)^2}{1 + \left(\tan\frac{\theta_2}{2}\right)^2}\right)K_2 + \left(\frac{2\left(\tan\frac{\theta_2}{2}\right)}{1 + \left(\tan\frac{\theta_2}{2}\right)^2}\right)K_3$$

Simplifies to;

$$(K_1 + K_2)\left(\tan\tfrac{\theta_2}{2}\right)^2 = 2(K_3)\left(\tan\tfrac{\theta_2}{2}\right) + K_2 - K_1 \quad (3.5)$$

From (3.5) θ_2 computed solving the quadratic equation as follows;

$$\theta_2 = \tan^{-1}\left(\frac{2(K_3) \pm \sqrt{4(K_3)^2 - 4(K_1)^2 + 4(K_2)^2}}{2(K_1 + K_2)}\right)$$

The quadratic formulae give two roots ± as there are potential, two answers (one where the links cross, and over where they do not.) The above equations enable us to calculate positions of P_2 and P_3 as shown below.

$$P_{0x} = 0$$

$$P_{0y} = 0$$

$$P_{1x} = L_1$$

$$P_{1y} = 0$$

$P_{2x} = L_2 \cos\theta_1$

$P_{2y} = L_2 \sin\theta_1$

$P_{3x} = L_1 + L_3 \cos\theta_2$

$P_{3y} = L_3 \sin\theta_2$

Point P_4 calculated as follows:-

Initially calculating L_7 length using co-sine rule;

$$L_7 = \sqrt{{L_1}^2 + {L_3}^2 - (2)(L_1)\,(L_3)\cos(\pi - \theta_2)}$$

Finding angle μ;

$$\mu = \cos^{-1}\left(\frac{{L_7}^2 + {L_4}^2 - {L_2}^2}{2(L_7)(L_4)}\right)$$

$$\beta = \mu + 0.45 \qquad (3.6)$$

In (3.6) 0.45 rad angle between L_5 and L_4 was a constant angle (26 degrees) added for β angle calculation.

For L_8 calculation co-sine rule;

$$L_8 = \sqrt{{L_5}^2 + {L_7}^2 - 2(L_5)(L_7)\cos\beta}$$

Hence, from co-sine rule again;

$$\varphi = \cos^{-1}\left(\frac{{L_2}^2 + {L_8}^2 - {L_6}^2}{(2)(L_2)(L_8)}\right)$$

Angle made with L_8 and x-axis;

$$\emptyset = \emptyset_1 - \varphi$$

Hence, P4 coordinates;

$P_{4x} = L_8 \cos\emptyset$

$P_{4y} = L_8 \sin\emptyset$

3.3 Design of thumb

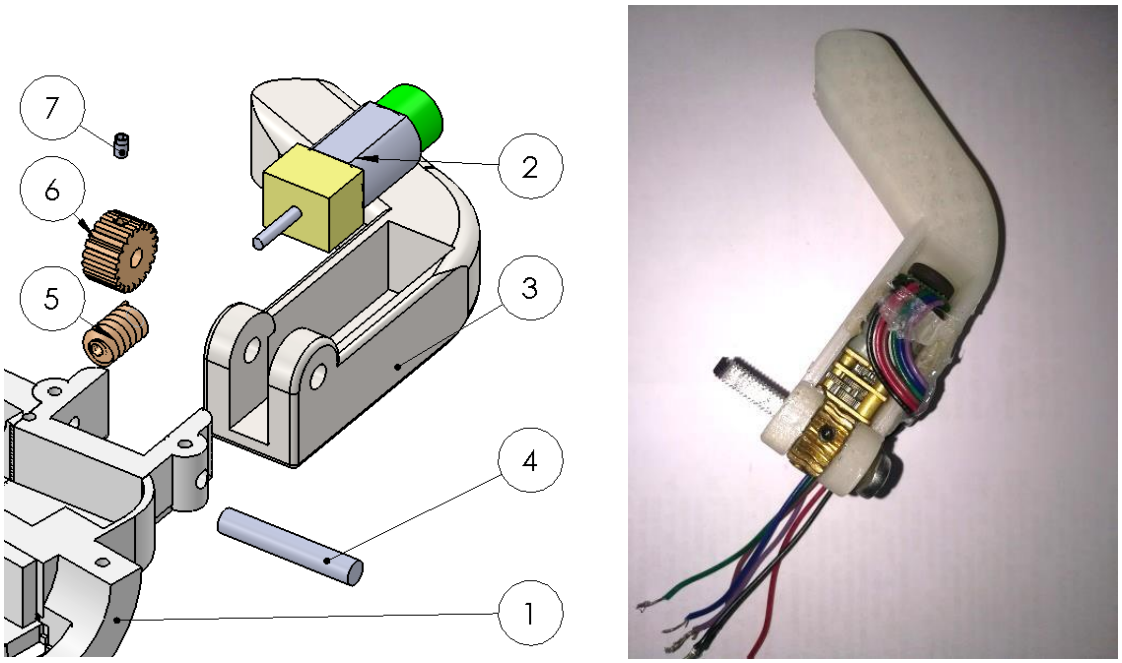

(a) **(b)**

Figure 3.5 (a) 3D model and (b) actual prototype developed for under-actuated prosthetic hand

Table 3.2 Components of thumb finger assembly with reference to Figure 3.5

Part no	Part Name	Function
1	Palm bottom housing	Houses main components and finger connections
2	DC gear motor with encoder	This motor actuates thumb flexion and extension and tracks thumb position with built-in encoder feedback.
3	Thumb motor housing	Thumb, finger structure and house components such as motor for actuating thumb flexion and extension movement.
4	Thumb pin	Connects motor housing and palm bottom housing via pin that is fixed to palm bottom housing.
5	Worm rod	Worm rod connects to the motor shaft and transmits motion
6	Worm wheel	The worm wheel is fixed to thumb housing bottom and once rotated entire assembly rotates along.
7	2mm Alan bot	Fixes to worm wheel to thumb pin as one solid component.

The thumb working principle is very simple when compared with other fingers since it activates directly via DC gear motor and gears. As shown in Figure 3.5 and Table 3.2 an exploded view shows how the components are interconnected. DC motor fits into the thumb motor housing and acts as one, worm rod press fits into the motor shaft. Worm wheel connects to thumb pin as one solid unit with 2mm Alan bolt, thumb pin connects to palm bottom housing. Once the motor actuates worm rod will revolve round fixed worm wheel

moving the thumb assembly. The thumb, finger range of motion was set to vary from 0 to 90 degrees.

Gear reduction analysis of thumb motion;

Gear ratio of motor = $\frac{GR}{1} = \frac{n_{out}}{n_{in}} = \frac{1}{298}$

Gear ratio worm gear = $\frac{GR}{1} = \frac{n_{out}}{n_{in}} = \frac{1}{20}$

Total gear reduction = $\frac{1}{298} \times \frac{1}{20} = 0.0002$

Total gear reduction calculates that for 2000 motor shaft revolutions only one revolution of worm rod.

3.4 Design of clutch module and cam shaft

Under-actuated mechanism mainly consists of two components; camshaft and clutch module. Many designs and trails led to finally achieve accurate and stable results of underacted mechanism. The initial design included two DC gear motors with encoders for thumb and clutch drive. For camshaft, motion transmission occurred through servomotor using belts and pulleys. Belts and pulley also transmitted motion for the clutch drive. Clutch actuation would occur for predefined servo motor rotation angles that eliminated the need of motor feedback. However, the problem with this implementation was with belts and pulleys that cause spillages. Therefore, gear wheels were set as a norm for motion transmission to avoid spillages and yield accurate motion transmission in design of underacted mechanism. Practical operations showed using a servo motor for camshaft movement was not suitable due to lack of feedback and torque requirement. Therefore, DC gear motor with inbuilt encoders was much suited.

The final design included gear wheels for motion transmission from motors to clutch plate with gear wheels inside the clutch module also. Inside the clutch module consists of plastic spur gears considering a suitable module of gears. Idler wheels between each clutch gear plate, which would ensure that all clutch gear plates, would rotate in one direction to one another. The use of worm gears for camshaft rotation avoided any backlash created from clutch engagement and disengagement. This clutch module prototype yielded better results when compared with earlier versions in terms of stability and accuracy. To obtain structural

rigidity of the clutch housing most of the clutch component materials included mild steel and aluminum for fabrication. During design iterations, addition of bearings for rotational components to minimize friction was important. Such areas include a male clutch plate and a housing back plate, also clutch plate with gear wheels and a clutch housing front plate. Considering limited space, selection of miniature bearings to match design parameters was crucial. The inner diameter of the bearings was 6mm, outer diameter 10mm and thickness of 3mm (bearing no: MR106ZZ).

The clutch mechanism consists of three major components, namely male clutch plate, female clutch plate and clutch plate with a gear wheel. Clutch plate with gear wheel transmits motion produced from motor. The female clutch plate consists of an output shaft that would transmit the rotational motion of the proximal finger via a worm gear mechanism. Male clutch plate pushes itself and the female clutch plate towards the clutch plate with gear wheel once camshaft rotates. In the clutch to be in engaged, interlocking pins of male clutch plates interact with clutch plate with gear wheels and female clutch plate, this stage is defined as clutch engaged. Once the DC motor rotates these three components rotates transmitting motion from motor to proximal finger worm wheel.

Figure 3.6 shows an exploded view of this clutch module and Table 3.3 indicates components and each component's functionality. The operating principle of this clutch mechanism was simple as it mimics a positive clutch type. One clutch consists of three parts that are a clutch plate with a gear wheel, a female clutch plate, and a male clutch plate.

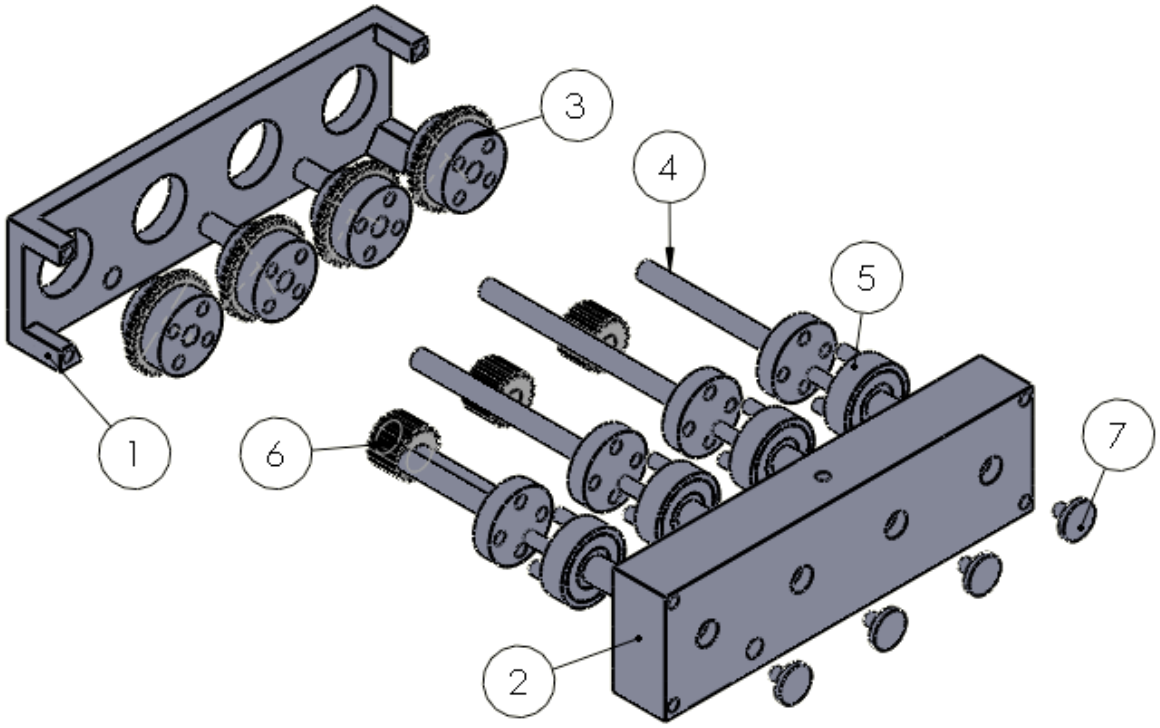

Figure 3.6 Components of clutch module

Table 3.3 Components of clutch module assembly with reference to Figure 3.6

Part no	Part Name	Function
1	Clutch housing front plate	Houses clutch components and idle wheels that fix into the internal wall of the clutch housing front plate.
2	Clutch housing back plate	Guides the clutch into the locking mechanism and houses the clutch module with a clutch housing front plate.
3	Clutch plate with gear wheel	Transmits motion into a clutch once the clutch is engaged.
4	Female clutch plate	The female clutch plate is the output of the clutch module to which shaft connects to the finger. The plate also consists of holes for clutch engagement.
5	Male clutch plate	This clutch plate consists of a miniature shaft that locks into a female clutch plate.
6	Idle gear wheels	These gear wheels ensure rotation of the clutch plate with gear wheels rotate in the same direction.
7	Spring return clutch engages pin	A mechanical link which links cam input and clutch actuation.

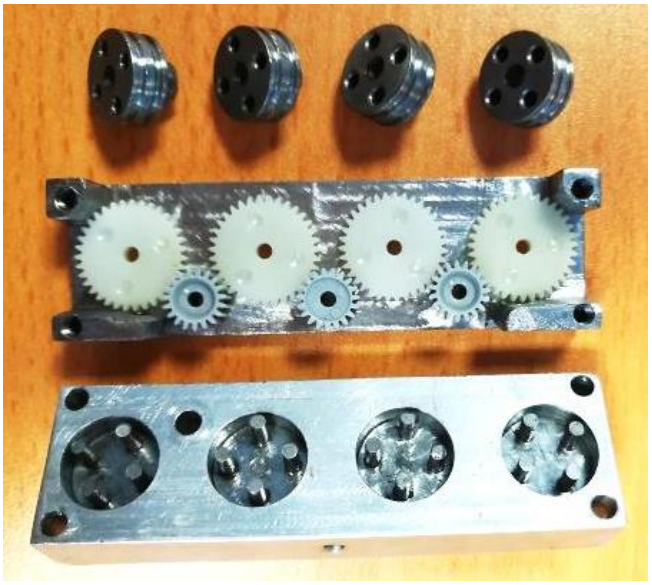

(a)

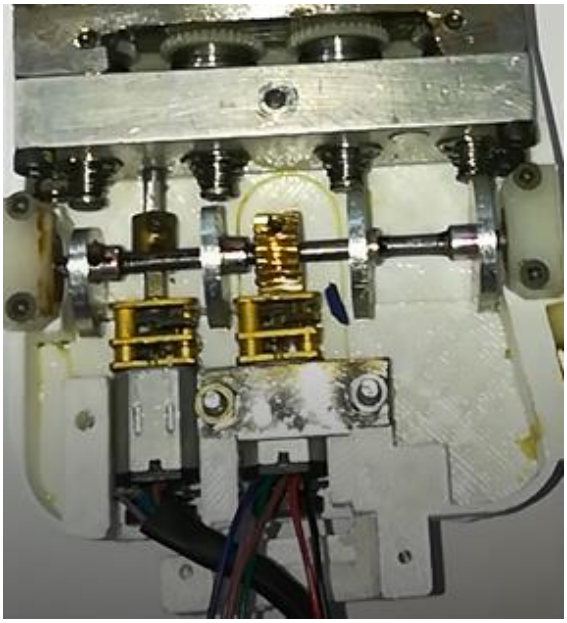

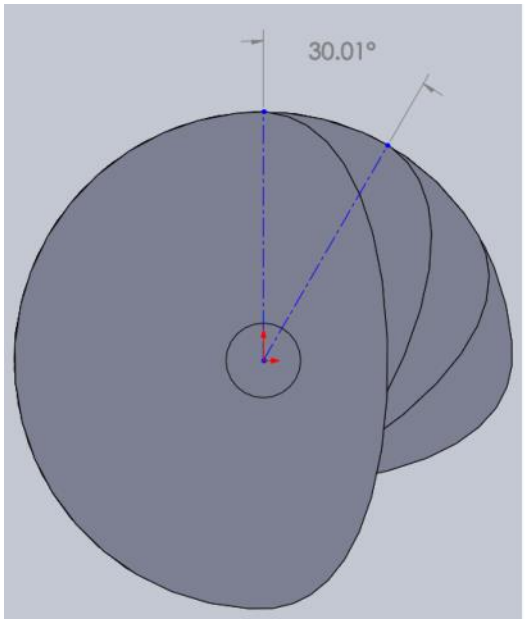

(b) **(c)**

Figure 3.7 (a) - gears placement and fabricated components of a clutch module (b) (c) - cam shaft module driven using worm wheel arrangement

Secondly, the most important component of the under-acted mechanism is the camshaft. Once camshaft rotates cams, will encounter spring return clutch engage pin of male clutch plate, which pushes the male clutch plate forward. Male clutch plate and push rod connected by a threaded screw, between clutches engage pin, and clutch housing back plate a conical spring is in place. This conical spring serves the purpose of driving the male clutch plate to its original position once the cam releases its contact with a clutch engages a pin upon rotation.

Conical springs instead of extension springs were more suited since; conical springs take less space once compressed. One key feature in the camshaft construction includes the manner in which each cam offsets from one another by 30 degrees. Rotation of the camshaft begins via a worm gear mechanism once its dedicated DC gear motor with encoder actuates. This enabled to reduce any backlash generated from the spring return push rod. Figure 3.7(a) shows the internal components during the assembly stage Figure 3.7 (b) shows how the camshaft and clutch module interacts. Figure 3.7(c) shows offset present in camshaft.

Gear reduction calculation for finger actuation;

Gear ratio of motor = $\frac{GR}{1} = \frac{n_{out}}{n_{in}} = \frac{1}{298}$

Gear ratio of clutch mechanism = $\frac{GR}{1} = \frac{n_{out}}{n_{in}} = \frac{35}{19}$

Gear ratio worm gear = $\frac{GR}{1} = \frac{n_{out}}{n_{in}} = \frac{1}{20}$

Total Gear Reduction = $\frac{1}{298} \times \frac{35}{19} \times \frac{1}{20}$ = 0.0003

For 3000 rotations of the clutch drive motor, the worm wheel at proximal finger rotates one revolution. For one rotation of the camshaft, its motor should rotate 2000 revolutions (same as thumb actuation).

3.5 Operational flow chart of prosthetic hand

The operation of the developed prosthesis consists of sequential steps to generate the final grip pattern. Let us consider an example of index finger flexion and extension;

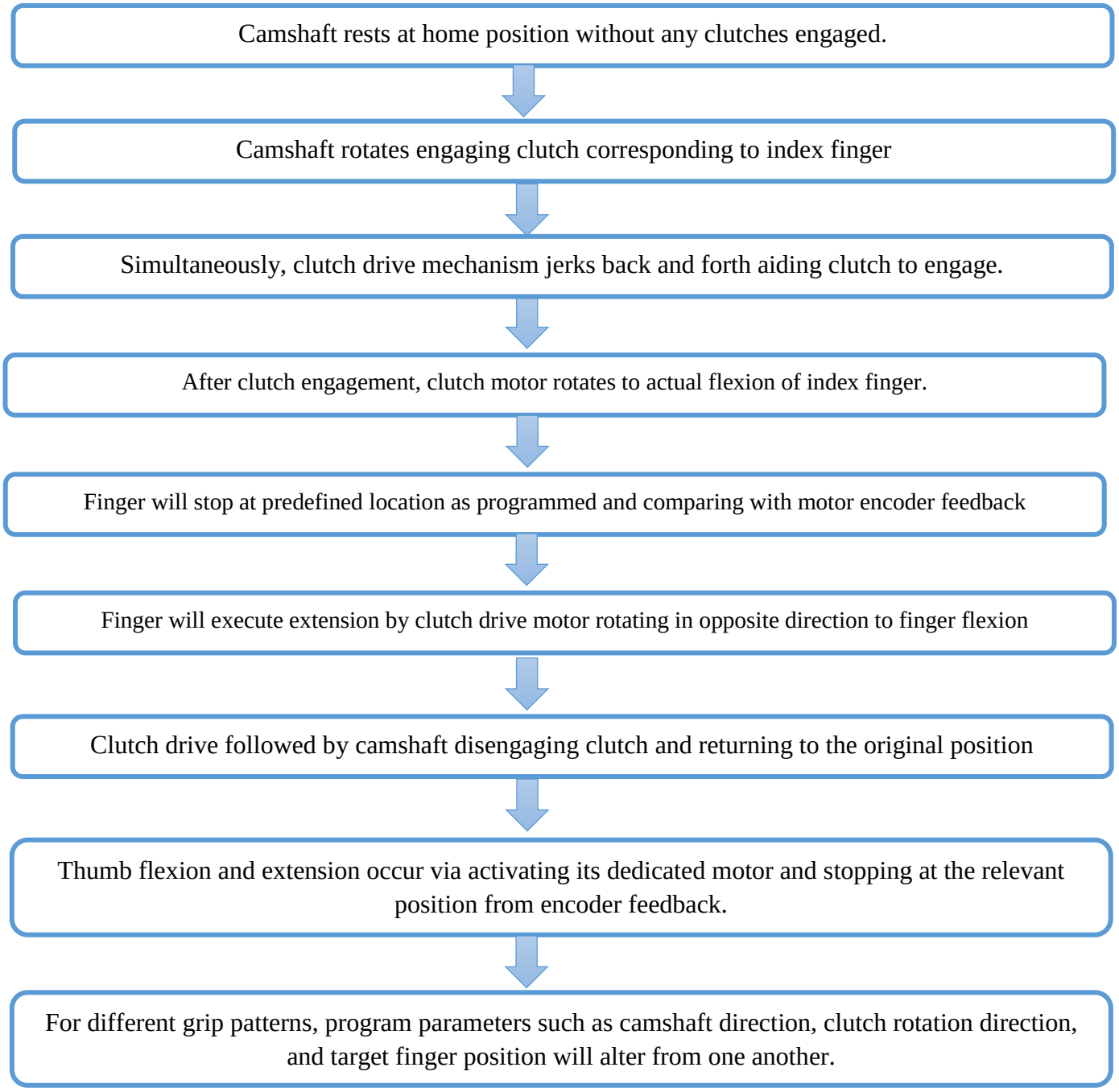

3.6 Fabrication of components

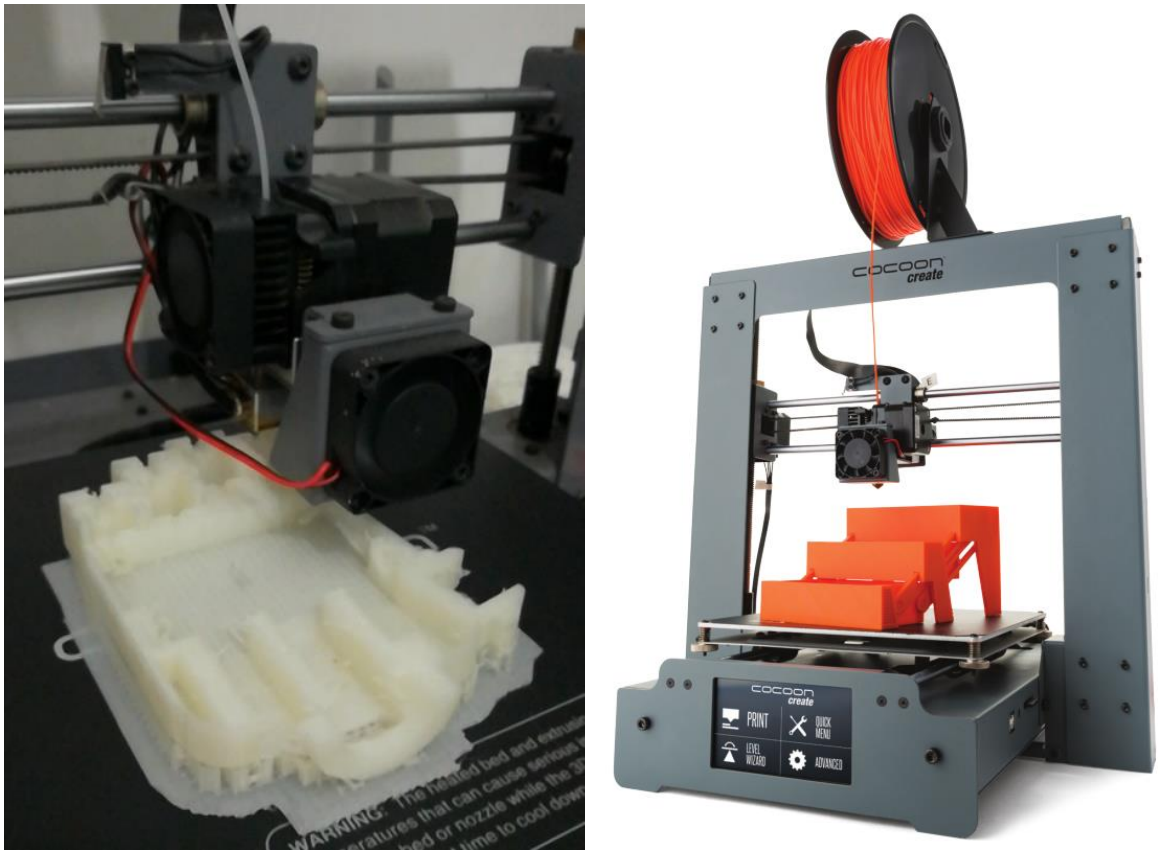

(a) **(b)**

Figure 3.8 (a) 3D printing of palm bottom housing (b) cocoon creates 3D printer

3D printing is a process whereby a real object created from a 3D design. Fused filament fabrication (FFF) is one of the most common technologies used by a 3D printer. To achieve this FFF works on an additive principle by laying down material such as PLA or ABS filament in layers to create 3D objects. Figure 3.8 shows the 3D printer in action.

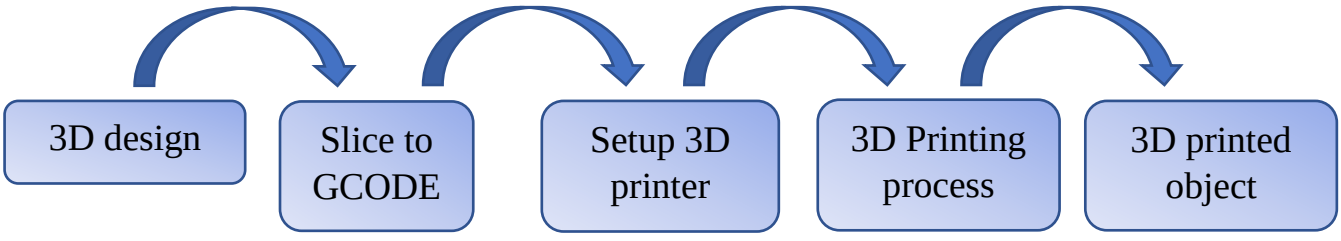

Figure 3.9 Stages from 3D design to printed 3D object

Table 3.4 Specification of 3D Printer

Printing	Description
Print technology	Fused Filament Fabrication (FFF)
Build volume	200 x 200 x 180 mm
Layer resolution	0.1 – 0.4 mm
Positioning Accuracy	X 0.012 mm
	Y 0.012 mm
	Z 0.004 mm
Extruder Quantity	Single Extruder
Extruder Diameter	0.4 mm
Print Speed	10 mm/s – 70 mm/s
Travel Speed	10 mm/s – 70 mm/s
Temperature	
Ambient Operating Temperature	15 – 30 (degree celcuis)
Operational Extruder Temperature	170 – 260 (degree celcuis)
Operational Print Bed Temperature	30 – 120 (degree celcuis)
Software	
Slicer software	Cura
Cura input format	.STL,.OBJ,.DAE,.AMF
Cura output format	.GCODE

3D printing technology using Polylactic acid (PLA) filament was the base for fabricating majority of components in this proposed build. This allows for lowering the overall weight of the hand. Secondly, the precise components present in the clutch module was fabricated using CNC machines to achieve high functional accuracy. 3D models developed using CAD software saved as STL (stereo-lithography) format; this conversion splits the object layer by layer. The 3D printer reads every slice and creates the object layer by layer gradually building the final object. 3D printing material used was PLA white color with 1.75 mm filament diameter. One of the most complex parts of 3D print was the palm bottom housing. This single piece along requires 22 hours of print time due to design complexity. The secondary process of 3D printing included cleaning of surfaces and removing support structure that ensures a perfect fit. Cams present in the camshaft was CNC machined to achieve even cam profiles. Aluminum for cams was a better choice considering its metallurgical properties and machining convenience. Table 3.4 lists the specifications of the 3D printer used.

(a) **(b)**

Figure 3.10 (a) machined aluminum cams (b) CNC machining process

Cam profiles were machined as one single piece that later was cut into four equal pieces as shown in Figure 3.9(a). The camshaft consist of a 3mm mild steel shaft and the cams were assembled paying special attention to even space and offset angle between the cams. Due to the miniature dimensions of components, special jigs for holding the workpiece aided the CNC machining stage as shown in Figure 3.9 (b). Assembling these components required attention to detail considering the cost for fabrication of under-actuated mechanism components. For finger assembly connecting links, proximal phalange, and distal phalange 2mm, 3mm and 4mm bolts aided for a sufficient connection.

3.7 Control hardware

Due to the implementation of under-actuated mechanism electronics present in this robotic prosthetic hand are comparatively less complex. The prosthetic hand consists of three actuators that are 12V DC gear motors with Hall Effect encoders. For experimental setup, motor controlling and encoder feedback were processed using microcontroller (Arduino, ATmega 2560) and dual H-bridge motor drivers. From trial and error thumb position, clutch drive, and cam drive was recorded using encoder feedback and included in the final program. During the experimental setup, the EMG sensor was not included, but its serial monitor fed inputs mimicked flex signals.

3.7.1 DC gear motor

These micro gear motors are incredibly tough and feature full metal gears. They have a gear ratio of 298:1, operate up to 12 volts and have a stall torque of 70 oz-in. with a max speed of 90 RPM. Each micro gear motor has a 3mm D-shaft. Appendix B describes more on the specifications of this motor.

3.7.2 Motor driver

The L9110 2-Channel motor driver module is a compact board that drives small robots. This module has two independent motor driver chips that can each drive up to 800mA of continuous current. The boards can be operated from 2.5V to 12V enabling this module to be used with both 3.3V and 5V microcontrollers. A PWM (Pulse Width Modulation) signal controls the speed of a motor and direction changes by changing polarity. Appendix C describes more of the specifications of this motor driver.

3.7.3 Microcontroller

The Arduino Mega 2560 is a microcontroller board based on the ATmega2560. It has 54 digital input/output pins (of which 15 can be used as PWM outputs), 16 analog inputs, 4 UARTs (hardware serial ports), a 16 MHz crystal oscillator, a USB connection, a power jack, an ICSP header, and a reset button. The integrated development environment provided by Arduino enables to program the onboard microcontroller. Figure 3.10 and Table 3.5 illustrate more information about the microcontroller.

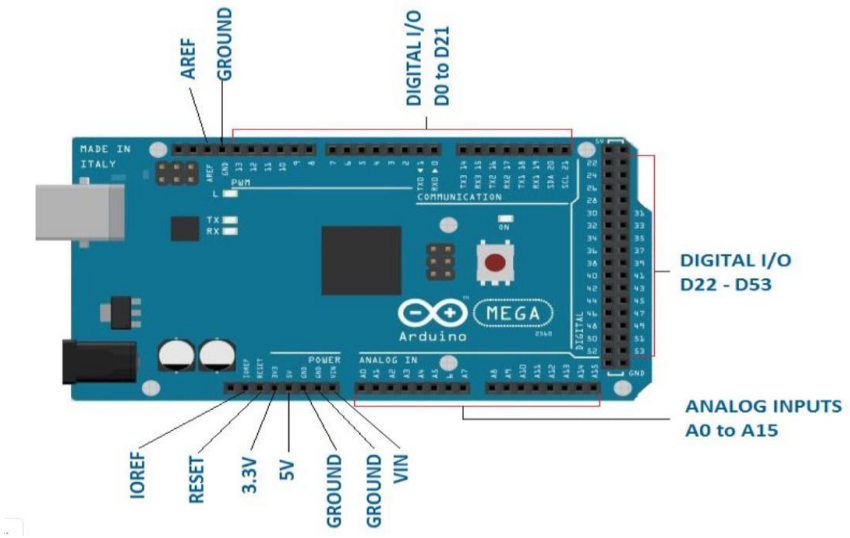

Figure 3.11 Overview of Arduino Mega microcontroller

Table 3.5 Arduino Mega specifications

Description	Valve
Microcontroller	ATmega2560
Operating voltage	5V
Input voltage	7-12 V
Input Voltage (limits)	6-20V
Digital I/O Pins	54 (of which 15 provide PWM output)
Analog Input Pins	16
DC Current per I/O Pin	40 mA
DC Current for 3.3V Pin	50 mA
Flash Memory	256 KB of which 8 KB used by boot loader
SRAM	8 KB
EEPROM	4 KB
Clock Speed	16 MHz
USB Host Chip	MAX3421E
Length	101.52 mm
Width	53.3 mm
Weight	36 g

3.8 Control algorithm

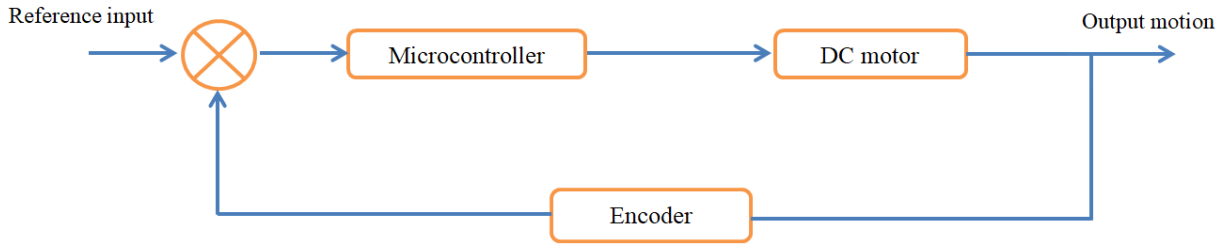

Figure 3.12 Closed loop control system for a prosthetic hand

The prosthetic hand control system consists of a motor encoder feedback for position tracking of fingers, hence this is a closed-loop control system. Figure 3.11 depicts how the closed-loop control system works with the test setup. The reference input is fed into the microcontrollers via Arduino's serial monitor. The microcontroller sends the signal to the motor driver which actuates the motor. DC gear motor's motion is tracked via an inbuilt motor encoder which is the feedback component in the closed-loop circuit. Once feedback encoder values match with predefined value programmed to microcontroller motors will halt and execute as programmed. Figure 3.12 shows a serial interface for prosthetic hand control and Table 3.6 shows the command and outcome of the command.

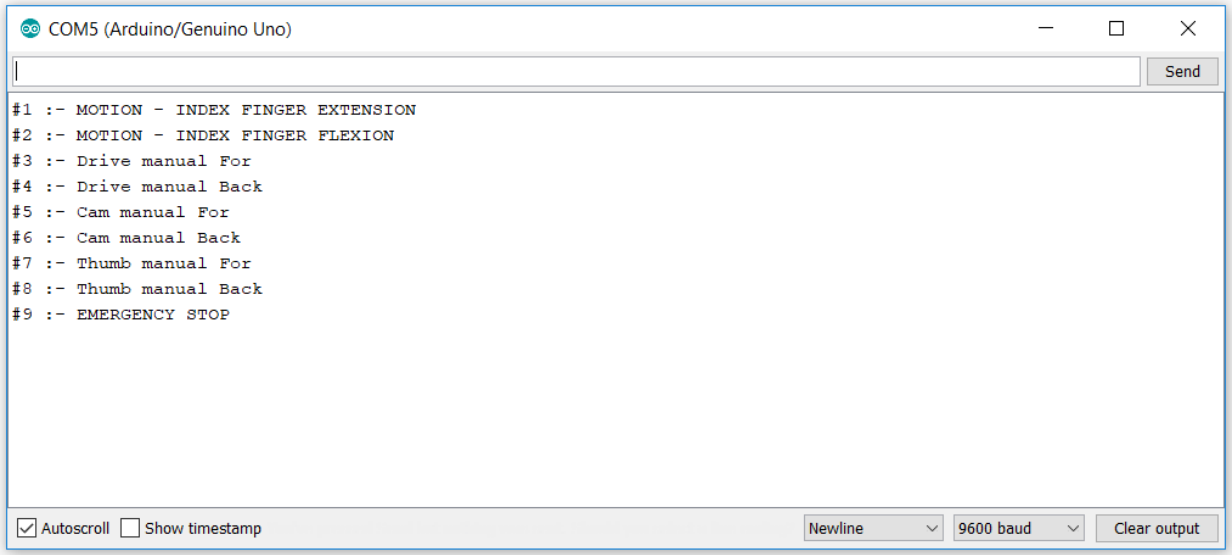

Figure 3.13 Serial interface for prosthetic hand control

Table 3.6 Commands and outcome of command

Command	Outcome
Motion – Index Finger extension	Executes pre-programmed index finger extension actuating camshaft motor, drive motor and thumb respectively.
Motion - Index Finger Flexion	Executes pre-programmed index finger extension actuating thumb, drive motor and camshaft motor respectively.
Drive manual For	The drive gear motor will rotate in a clockwise direction until “EMERGENCY STOP” is entered.
Drive manual Back	The drive gear motor will rotate in anti-clockwise direction until “EMERGENCY STOP” is entered.
Cam manual for	Cam motor will rotate in a clockwise direction until “EMERGENCY STOP” is entered.
Cam manual back	Cam motor will rotate in a clockwise direction until “EMERGENCY STOP” is entered.
Thumb manual for	Manually thumb could be operated forward (extension).
Thumb manual back	Manually thumb could be operated backward (flexion).
EMERGENCY STOP	Shuts down power to all motor drives disabling motors.

This experimental setup enabled observe mechanical disturbances such as worm wheel backlashes and mechanical limitations of different grip patterns. One downside of this control system is the position of the figure is derived relative to the motor and not finger position. This derivation of the finger position relative to the motor is prone to generate error even in the presence of minimizing mechanical disturbance. For example, once the prosthetic hand performs grasping action on an object, the required amount of grasping force might not be delivered to the proposed prosthetic hand design. The position of fingers and the amount of force required to grasp various kinds of objects are considered to be developed under future works.

CHAPTER 04 : SIMULATION AND EXPERIMENTS

Simulations, experiments and analysis gave more insight about the developed hand exploring its operation and limitations. Solidworks computer aided design tool build model of prosthesis hand from the start. The inbuilt motion study feature in Solidworks showed that the expected motion patterns of fingers before physically building the prototype. The kinematic model developed for finger actuation discussed in chapter 3.2: kinematic analysis of finger fed into a Matlab program. This shows how links and joints moved in space that shows the area occupied by fingers during flexion and extension.

4.1 Solidwork simulations

Solidworks simulation employs a generative method for support of design optimization. Design variables vary between their respective lower and upper bounds. These design variables combined to create individual design scenarios. Various simulations carried out for all scenarios generated. Among the scenarios, evaluated feasible designs collected and within the feasible designs. The best design that yields the lowest value in the objective function identified as the solution to the design problem.

4.1.1 Solidworks motion analysis

During this under-actuated robotic prosthesis design, it was required to understand the kinematics and dynamics before building physical prototypes. Motion simulation also known as rigid body dynamics offers a simulation approach for solving these issues. The mechanism was simulated applying predefined, arbitrary actuation angles provided by the rotary motors, with the motion study tool of the software package. For smooth motion, the path of the fingertips and thumb recorded. Figure 4.1 shows developed model under Solidworks motion analysis.

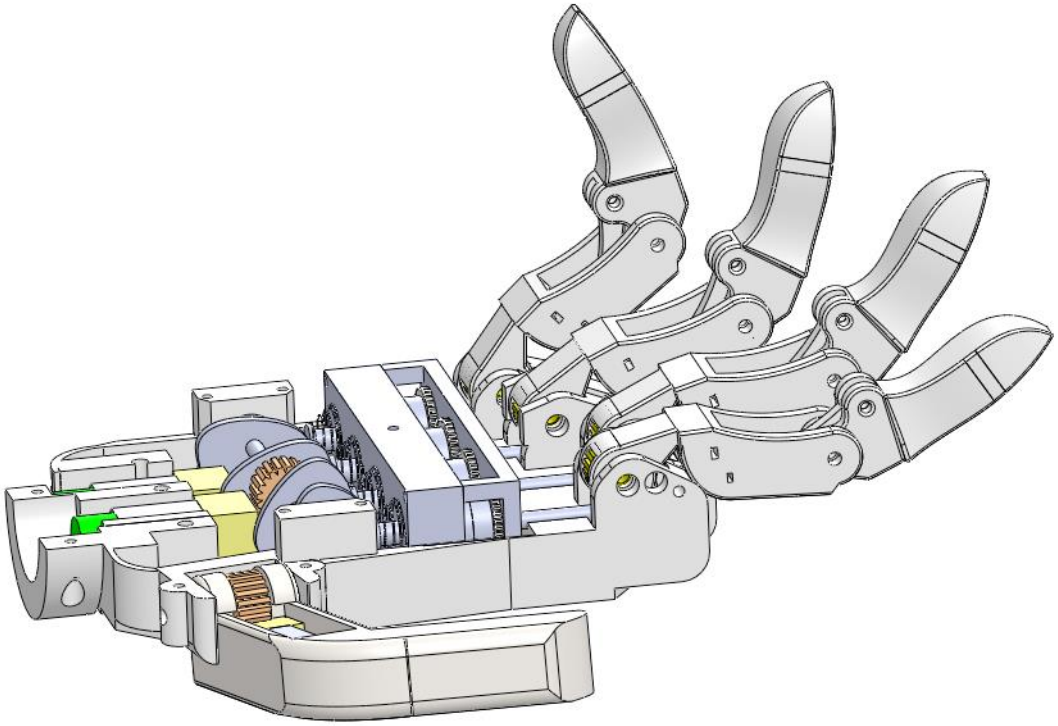

Figure 4.1 Solidworks motion simulation in action

4.1.2 Solidwork camshaft simulation

The camshaft is a critical component of this under-actuated mechanism. The camshaft model consists of an offset of 30 degrees between each cam. This offset arrangement yielded the best results of clutch engagement and disengagement. It was critical in the assembly stage to maintain this 30-degree offset between each cam. Figure 4.2(a) depicts the final CAD version of camshaft. The shape of the cam was critical to determine the rise and dwell times of the follower. Generation of cam displacement profile was possible through solidworks software. Figure 4.2(b) shows the individual cam displacement profiles graphed into a single graph to visualize how cams would engage clutches.

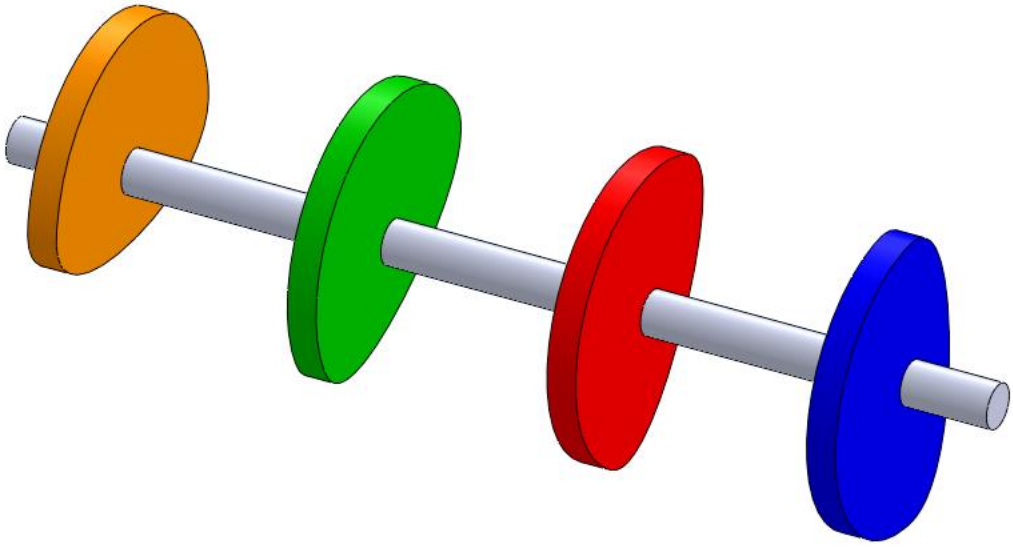

(a)

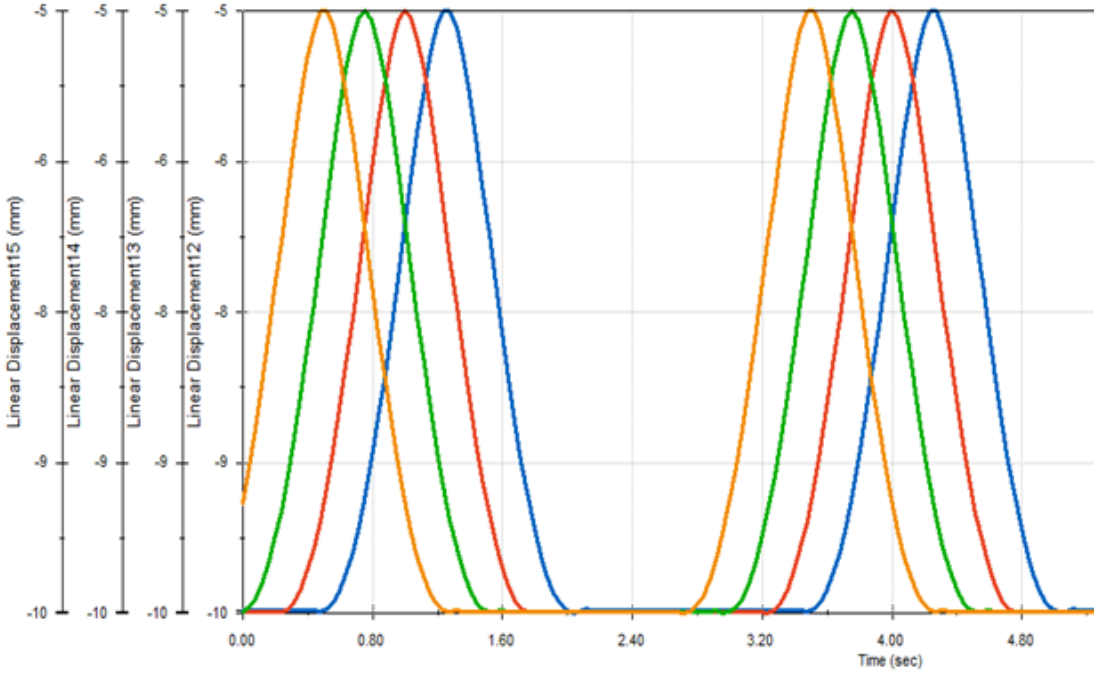

(b)

Figure 4.2 (a) Designed CAD model and machined cam shaft. (b) Linear displacement of individual CAM profiles for each finger

From the above linear displacement graphs, the displacement of the follower was essential to design proper dimensions of the clutch module. This distance was critical in designing a precise clutch module, which ultimately eliminates any jerks in motion transmission. In addition, this simulation helped to identify and develop better cam shape that results in proper clutch actuation. Initially designed cam profile had problems in cam shape that caused jerks in motions hindering clutch performance.

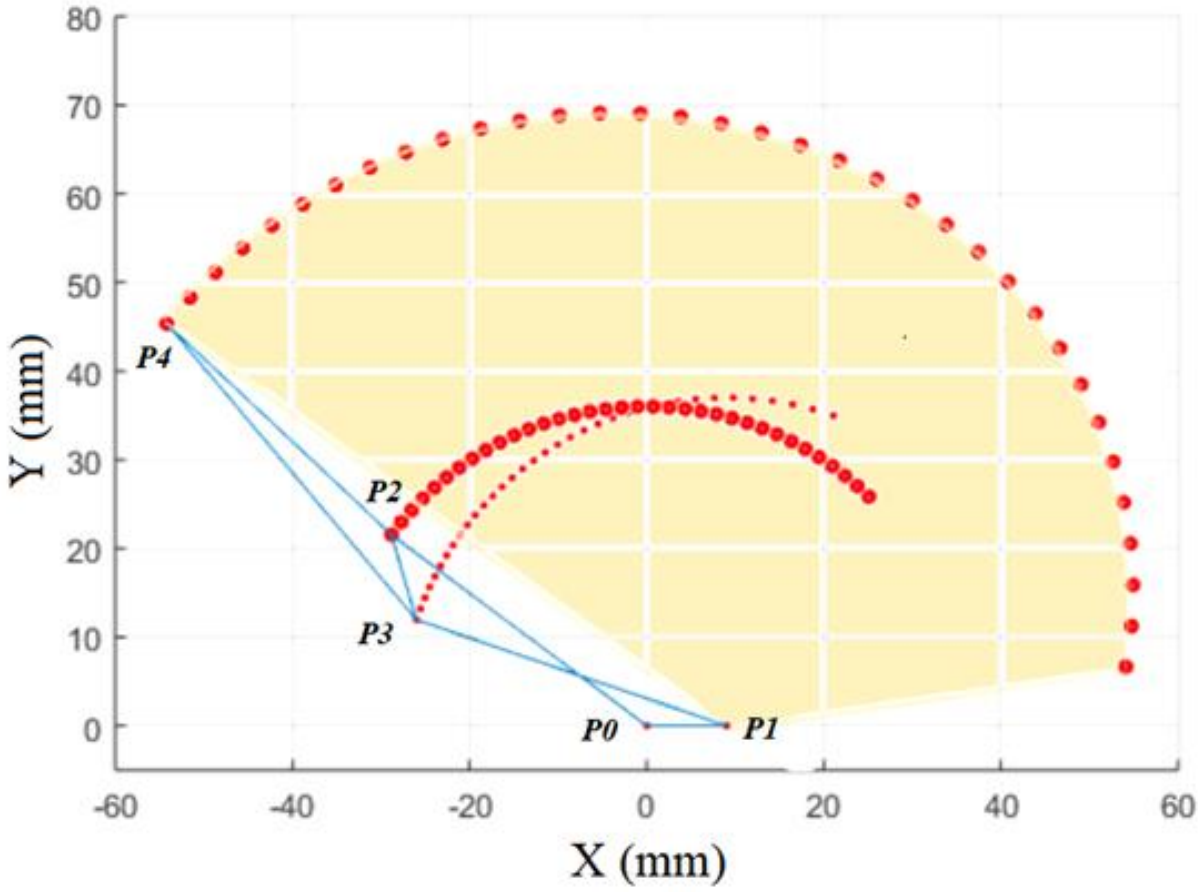

Figure 4.3 Finger workspace and finger point trajectory produced by Matlab software

A mathematical model discussed in chapter 3.2: kinematic analysis of finger design derives the kinematic model. Matlab software processed the model that graphically simulated workspace as well as joint and finger trajectory. Specifically this model was able to plot the finger trajectory of the distal fingertip and PIP joint variations with input MCP joint angle. Figure 4.3 shows such a plot using Matlab and shaded area shows the workspace of finger for flexion and extension.

4.2 Experiments

This chapter explores the methodology on how experimental results justify the objectives of this research. The experimental setup consists of a simple arrangement to generate results. The setup consisted of developed prosthesis hand that consists of an under-actuated mechanism along with actuators and finger mechanism. Electronics and control system were discussed in detail under chapter 3.7 about individual components used. Figure 4.4 shows an outline of an experimental setup that enabled to test and control developed under-actuated robotic prosthesis hand.

4.2.1 Analysis of under-actuated mechanism

An analysis of under-actuated mechanism was carried out to investigate force generated from a single finger (index finger) using a force scale. Current sensors measured the current drawn from DC gear motors present in the underacted mechanism. Maximum force produced by the finger corresponds to the rated maximum current DC motor draws. Secondly, to analyze underacted mechanism's performance comparison for MCP joint angle with motor revolutions for ideal and actual was carried out.

4.2.2 Index finger force and motor current analysis

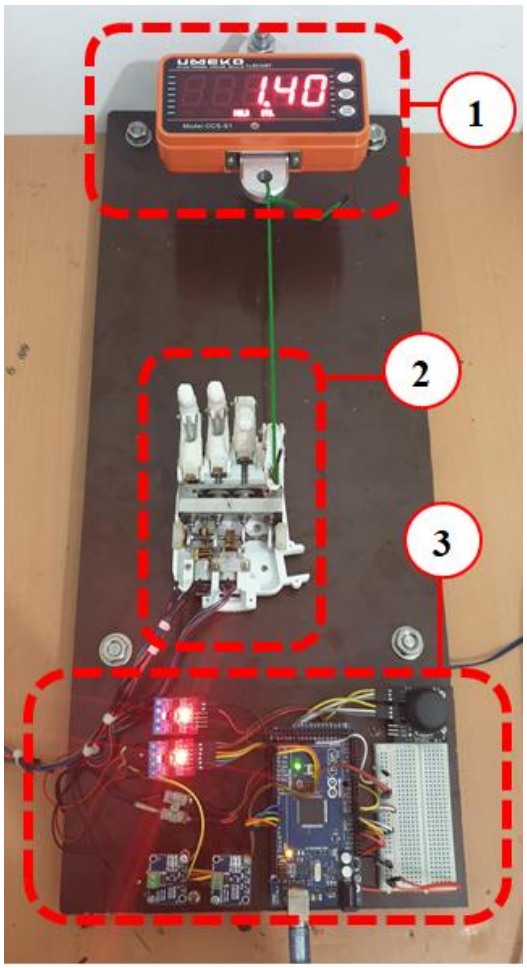

Figure 4.4 Experimental setup for index finger force measurement with motor current sensing. 1.Electronic force scale, 2. Prosthetic hand, 3. Electronic controls.

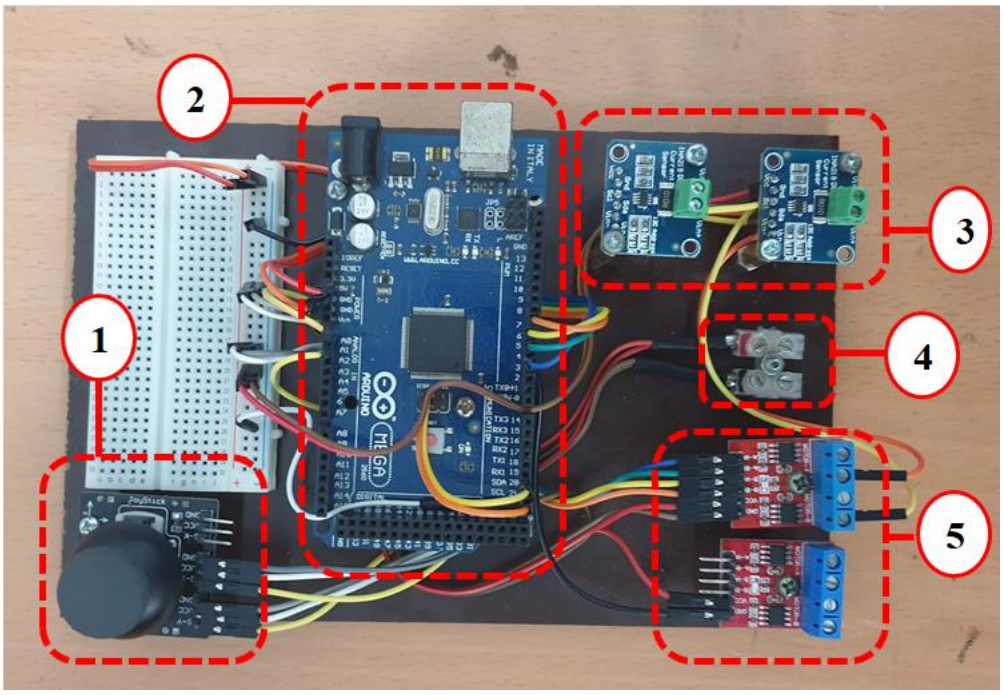

Figure 4.5 Electronic setup. 1. Joystick controller 2. ATmega 2560 microcontroller 3. Current sensors 4. 12v power input 5. Motor drivers

Figure 4.4 and figure 4.5 shows the setup to find the force produced from the index finger. This setup also measures the current drawn from each motor present in underacted mechanism (Camshaft motor and clutch drive motor). Maximum stall current of the motor is 1600 MA (Refer appendix B). Current sensors (INA219) in the electronic setup measure the current drawn from each motor. Current drawn from the clutch drive motor is plotted with time for single input from a joystick controller. For camshaft motor operation, measurement of current was in a similar fashion to investigate the performance of camshaft and clutch engagement.

As shown in Figure 4.6 current variation of clutch drive motor was plotted against time for index finger flexion. Point A shows the inductive spike generated from motor initially and point B shows the current drawn for clutch actuation and finger flexion under no tension load. Point C shows the finger pulling the wire with increasing tension, increasing the force thus increasing the motor current. Point C corresponds to the maximum force the finger produced with the maximum current of (1580 mA). Point D shows the motor stopped and motor traveling in the reverse direction to execute finger extension.

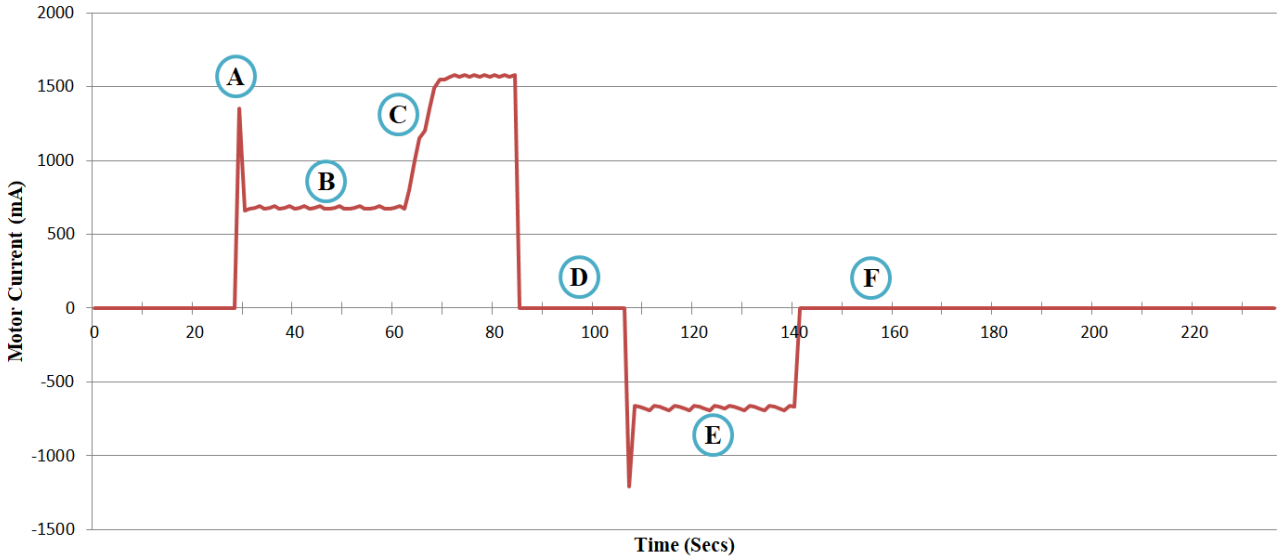

Figure 4.6 Current variation of the clutch drive motor with time

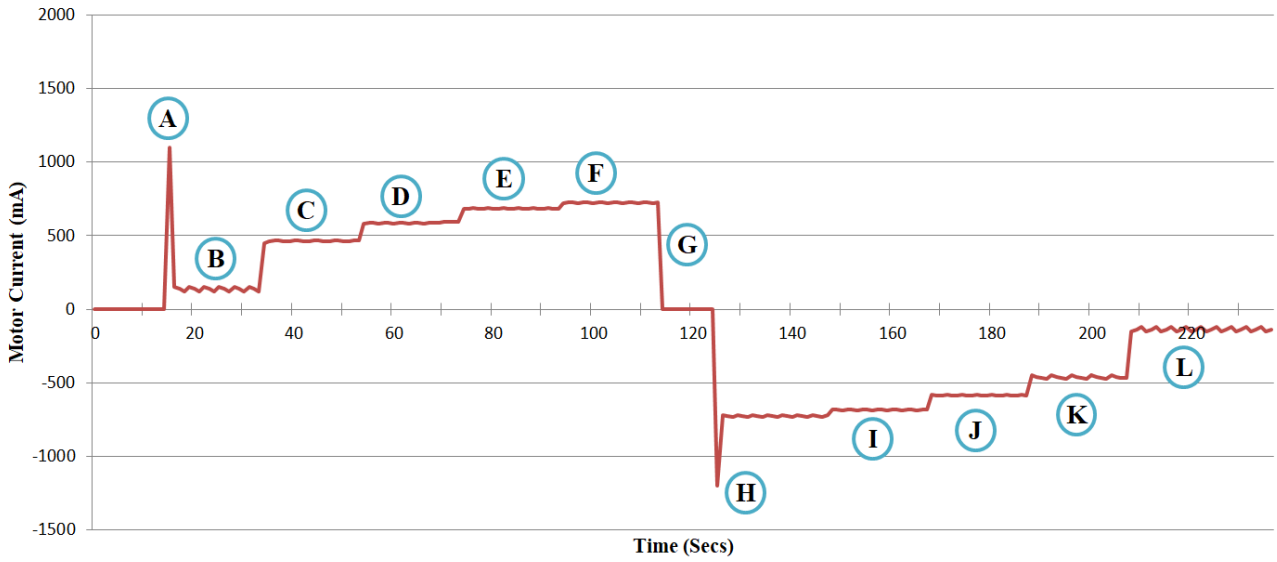

Figure 4.7 Current variation of camshaft motor with time

Figure 4.7 shows the current variation of camshaft motor with respect to time for clutch engagement of all fingers. Points A and H represents initial inductive spikes produced by the motor. Point B corresponds to motor travelling under no clutch engagement followed by point C. At point C, first clutch engagement happens causing more current drawn from the motor. As clutches engage one after another, current drawn from motor increases incrementally from point C to point F. Points H to L shows the cam works in reverse direction dis-engaging the clutches one by one lowering current drawn from each step.

4.2.3 MCP joint angle with motor revolutions

Data of ideal and actual MCP joint angles against clutch drive motor rotations were gathered. For every 20 rotations of the clutch motor drive, ideal and actual MCP joint angle variation was a plot. From Solidworks CAD model and gear reduction ratios, ideal MCP joint angle was calculated. It is evident that MCP angle of flexion and extension is 65 degrees. The actual MCP angle was found using kinovea video capturing tool that enables to detect MCP angle for every 20 rotations of the clutch motor drive. Figure 4.8 shows such angle calculation from kinovea of starting and ending angle of the MCP joint.

(a) (b)

Figure 4.8 Kinovea angle analysis (a) Starting angle of MCP joint (b) ending angle of the MCP joint

From gear calculation as discussed in the previous chapter it is clear that theoretically for 3000 motor rotations, one rotation of the proximal worm wheel is produced. Therefore,

360 degrees → 3000 rotations

For 65 degrees = $\frac{3000}{360} \times 65$ = 540 rotations

Hence, for 65 degrees 540 rotations are required.

Table 4.3 shows the actual and ideal values obtained for MCP angle from 0 to 540 motor rotations of clutch drive. DC motor encoder tracks motor rotations that enabled to track the position of finger for every 20 rotations.

Table 4.1 : Actual and ideal MCP angle variation for motor rotations clutch drive

Motor Rotations	Actual MCP angle (Degrees)	Theoretical MCP angle (Degrees)
20	166	166
40	164	163.5
60	160	161
80	157	158.5
100	154	156
120	152	153.5
140	150	151
160	147	148.5
180	143	146
200	138	143.5
220	137	141
240	135	138.5
260	132	136
280	129	133.5
300	127	131
320	122	128.5
340	120	126
360	115	123.5
380	114	121
400	110	118.5
420	107	116
440	104	113.5
460	101	111
480	97	108.5
500	95	106
520	94	103.5
540	92	101

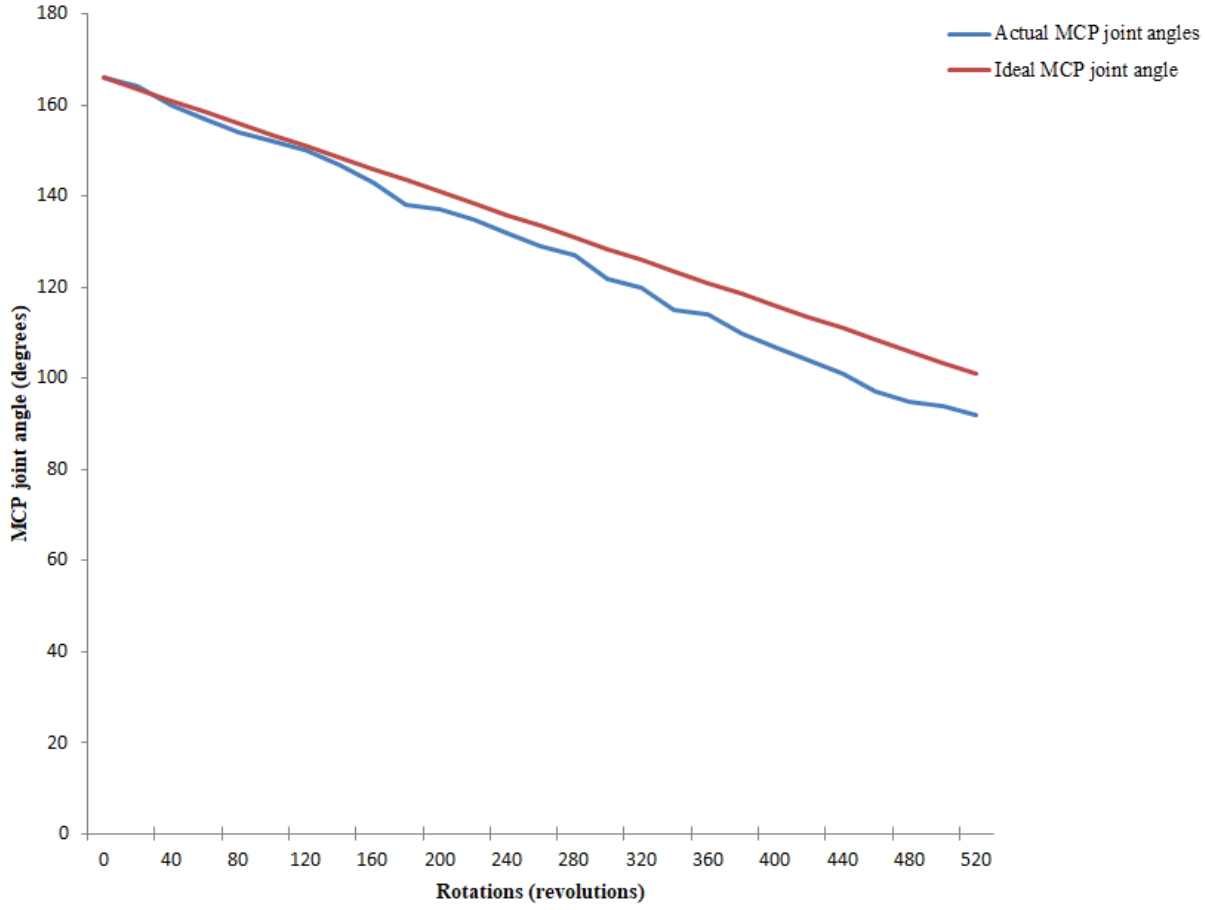

Figure 4.9 Actual and ideal MCP joint angle against clutch drive motor rotations

Figure 4.9 shows the variation in ideal and actual MCP angle observed for finite motor rotations. This shows that major variation is not present at the start, but slight variation observed towards the end where 9 degree offset is present. This variation might be due fabrication tolerances. However, this value is acceptable for under-actuated mechanism based prosthesis since major hindrance in grasping objects was not observed during experiments.

4.2.4 Setup and protocol

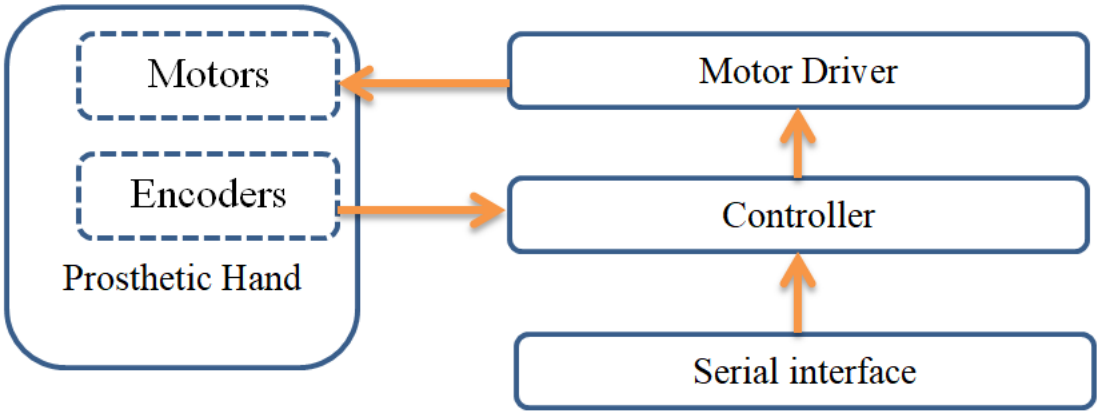

Figure 4.10 Experimental setup

4.2.5 Discussion

The objective of this study was to build an under-actuated mechanism that would achieve finger flexion and extension whilst having anthropomorphic features. Three gripping patterns, namely index finger extension; pinch grip and power grip served as test gripping patterns to mimic human hand movement. Using the experimental setup listed objectives and other various experiments were justified. During the development stage, start and end positions of flexion and extension of different gripping patterns were determined using encoder feedback via trial and error method. Microcontroller algorithm includes the reference values to define start and end positions of finger movement. Individual grip patterns underwent 20 cycles to ensure every time fingers would start flexion and extension from the same point. This confirms the system was within tolerances and no mechanical play hindered initial calibration of fingers that were set based upon encoder value.

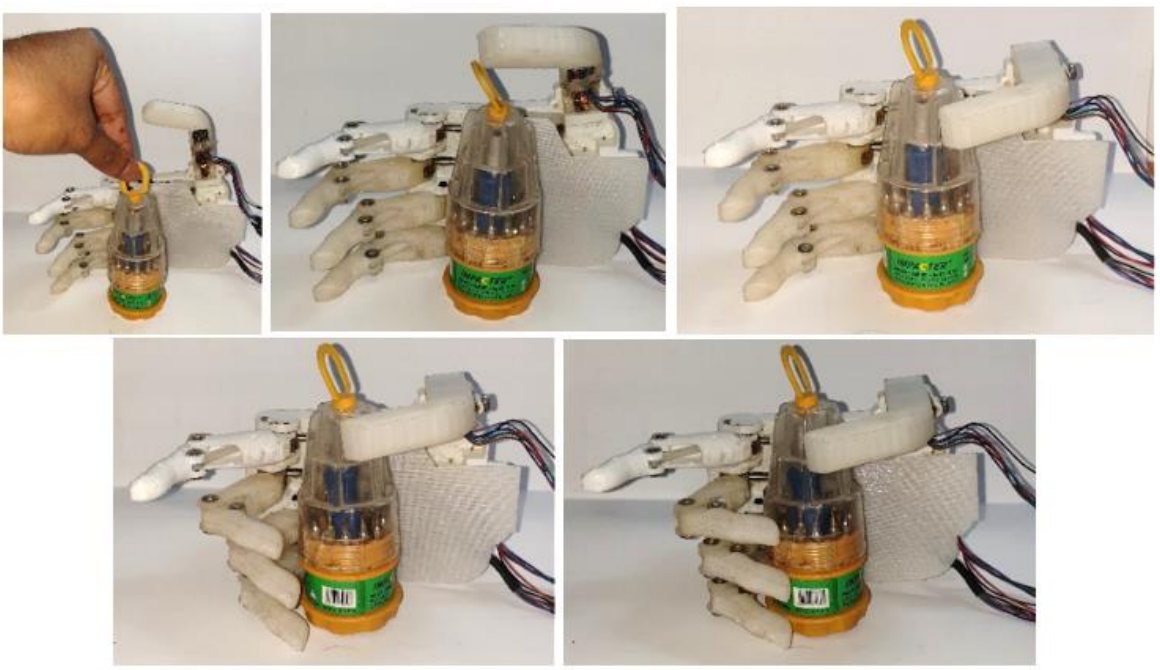

Figure 4.11 Snapshot of index finger extension

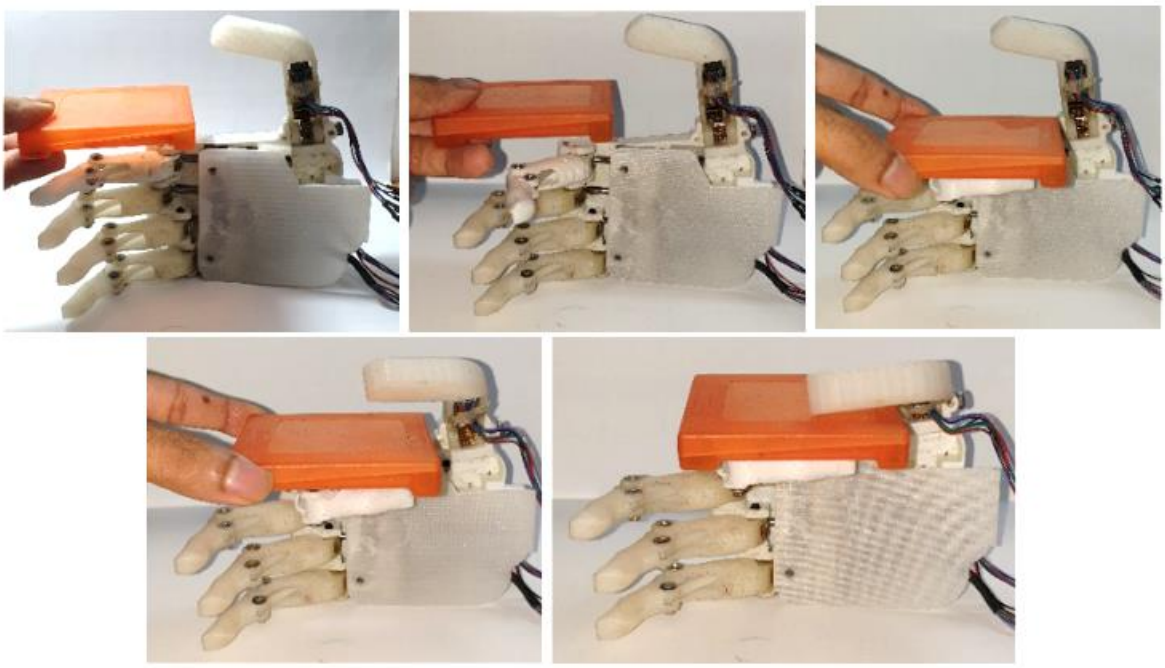

Figure 4.12 Snapshot of pinch grip

Figure 4.13 Snapshot of power grip

Using a microcontroller's serial monitor an interface to control prosthesis functionality was essential. This interface allowed to individually control each motor clockwise and anticlockwise and three defined finger gripping patterns index finger extension, pinch grip and power grip. Figure 4.11, 4.12 and 4.13 shows snapshots of prosthetic hand in action for index finger extension, pinch grip and power grip respectively.

Palmtop cover served as a protection during these tests to protect the internal mechanisms from grasping objects and to improve grip. Using power grasp pattern maximum payload of 1.4 kg was tested on prosthesis hand and this value was practically proved from an analysis carried out which is mentioned in future chapters. For all three defined grip patterns pinch grip, index finger extension and power grip measurement of time taken for a complete cycle of finger extension, flexion was important. Hence, an average reading of time recorded as shown in Table 4.1. This recorded time serves as a benchmark to improve on speed for finger flexion and extension; hence, the efficiency of clutch engagement and motion transmission developed for further works. Table 4.2 shows the specifications of developed prosthetic hand.

Table 4.2 Average time for finger movement

Action	Time duration for actuation		
	Pinch Grip	**Index finger extension**	**Power grip**
Time to Flex (secs)	12.78	13.3	13.05
Time to Extend (secs)	12.17	13.07	13.01

Table 4.3 Specifications of developed prosthetic hand

Specifications	Quality
Length of finger (mm)	80
Width of palm (mm)	73
Thickness of palm (mm)	26
MCP joint flexion range (degrees)	91 to 163
Degrees of freedom	5
No. of Actuators	3
Avg time to flex (seconds)	13.04
Avg time to extend (seconds)	12.75
Tested grasping patterns	3
Wight of prosthetic hand (grams)	900

Comparison of developed research hand with well-known commercially available prosthesis aided to get an idea about worth of research. Parameters considered in the comparison are the weight of the hand, the number of joints and the number of actuators used. These parametric values were a plot against each other for comparison purposes that is depicted in Figures 4.14, 4.15 and 4.16. For the weight of the prosthesis hand against the number of joints as shown in Graph 4.14 shows, developed hand U.A.A.R.P.H (under-actuated anthropomorphic robotic prosthetic hand) stands out from rest for higher weight also with a higher number of joints. Graph 4.15 shows the weight of prosthetic hand against several actuators, U.A.A.R.P.H seems to have a higher weight among all others, but less number of actuators when compared with bebionic and I limb versions. Graph 4.16 shows the number of actuators against the number of joints which stands out in the number of joints from others and low on the number of actuators when compared with other commercial prostheses.

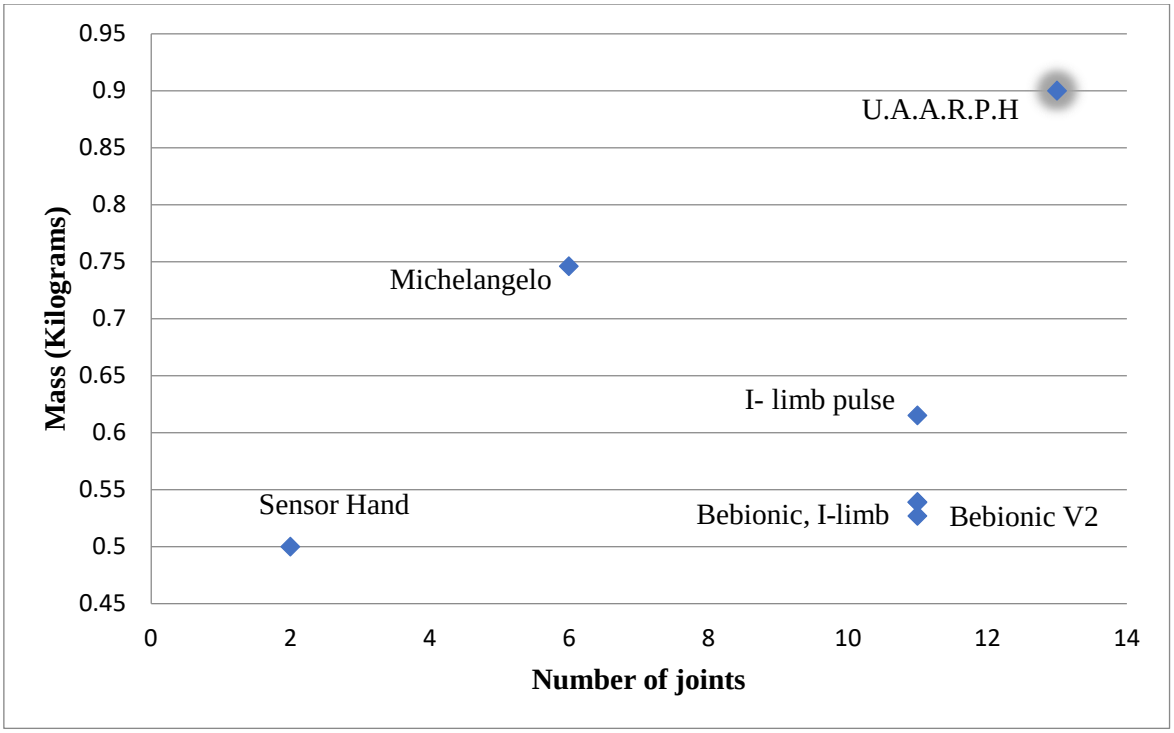

Figure 4.14 Mass of prosthesis hand against number of joints in each hand

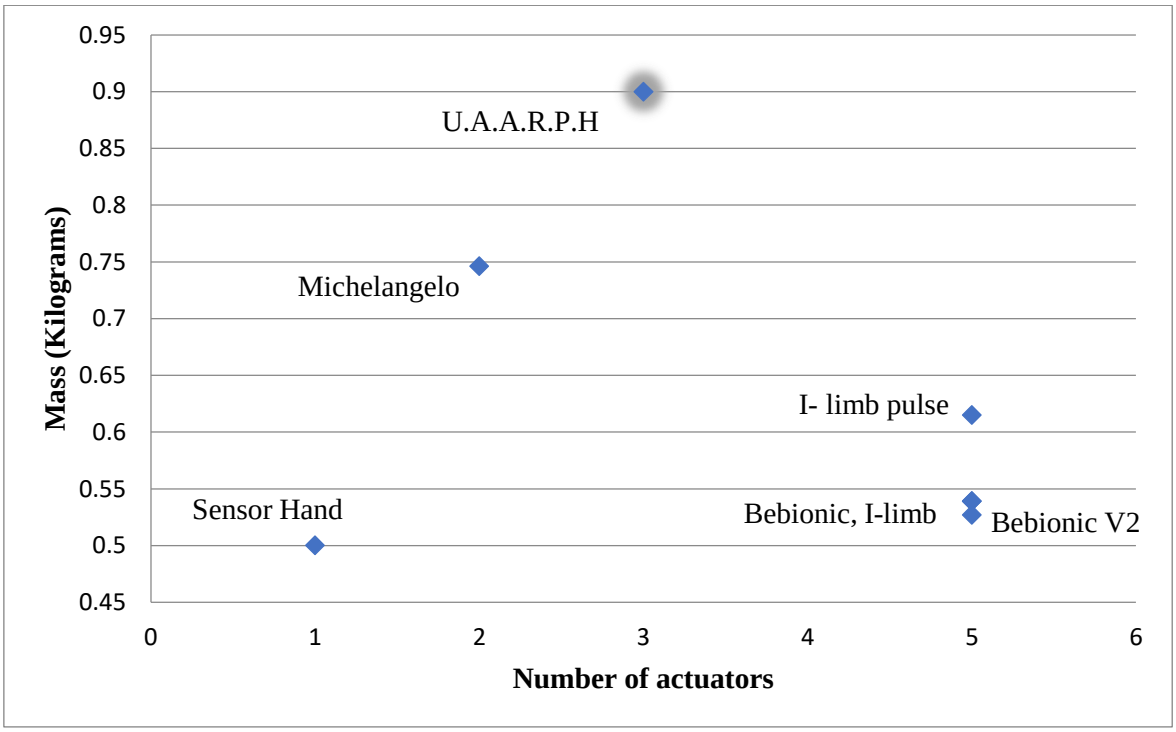

Figure 4.15 Mass of prosthesis hand against number of actuators in each hand

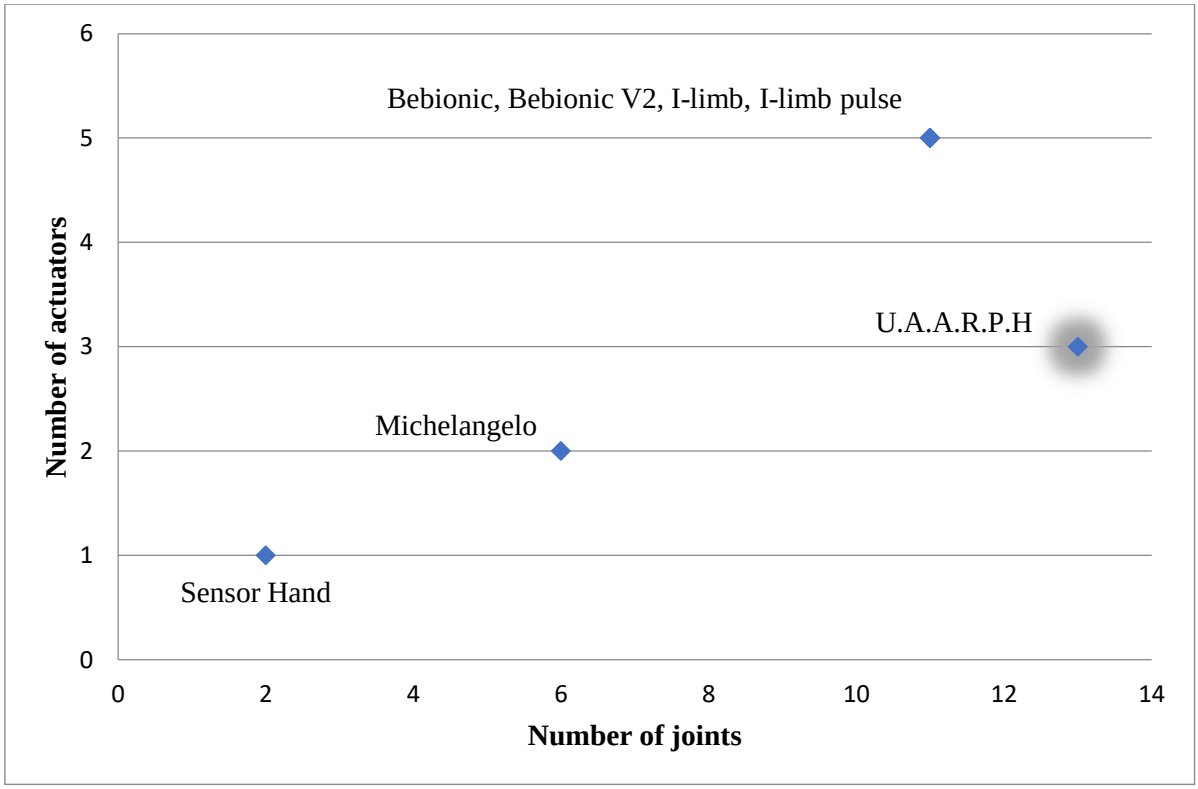

Figure 4.16 Number of actuators against number of joints in each hand

CHAPTER 05 : CONCLUSIONS

This thesis proposed an under-actuated anthropomorphic robotic prosthetic hand for trans-radial amputees. The developed prosthetic hand was designed using human anthropomorphic dimensions and an under-actuated mechanism that uses 3 motors to control flexion and extension of 5 fingers which consisted of 5 degrees of freedom. Using these design parameters 3D modeling software was used to design and optimize designs. Simulation and motion evaluations of designed prototypes were carried out to explore limitations and failures of a prosthetic hand. The kinematic analysis was carried out for modeled fingers that allowed visualizing finger motion using Matlab software to figure how joints would work to create the final workspace.

In fabrication, most components were fabricated using 3D printing additive manufacturing technology and CNC machining. Three design iterations were present throughout this product development to obtain stable under-actuated robotic prosthetic operation results. A critical component of this study was the under-actuated mechanism itself. This mechanism consists of a clutch module that was actuated by a camshaft. Once the mechanical components and motors were in place to test the functionality of the hand, the test setup was implemented. This assured that prosthesis hand functions as desired and accordingly, the algorithm was developed to test the functionality of the hand. The preliminary target of this project was to mimic three important gripping patterns using this under-actuated mechanism that are index finger extension, pinch grip, and power grip. Various tests were carried out to explore prosthetic hand's functionality and its limits. Analysis specifically related to under-actuated mechanism helps to identify its performance and limitations.

Future works of this project include controlling the hand using an EMG sensor replacing the computer control interface. This requires the fabrication of a prosthesis hand socket suitable for trans-radial amputees. Also planned to embed motor controllers, battery and controller inside this socket and move towards a lightweight compact design. Once an EMG sensor is included, control of this prosthesis hand could be carried out even to a higher stage. Apart from building a successful under-actuated mechanism, there is room for improvement.

PUBLICATIONS

1. R.P.D.D. Chamara and R.A.R.C. Gopura, “An Underactuated Mechanism for Anthropomorphic Robotic Prosthetic Hand” 5th International Conference on Control, Automation, and Robotics, Beijing, China, 2019, pp. 162 – 166.

REFERENCES

[1] D. S. V. Bandara, R. A. R. C. Gopura, K. T. M. U. Hemapala, and K. Kiguchi, "A multi-DoF anthropomorphic transradial prosthetic arm," in *5th IEEE RAS/EMBS International Conference on Biomedical Robotics and Biomechatronics*, 2014, pp. 1039–1044.

[2] "ISHN.com - the magazine for safety & health professionals who direct safety & health programs in high-hazard workplaces." [Online]. Available: https://www.ishn.com/. [Accessed: 22-Aug-2019].

[3] R. A. R. C. Gopura, K. T. M. U. Hemapala, and K. Kiguchi, *Upper extremity prosthetics: current status, challenges and future directions*.

[4] K. A. Raichle *et al.*, "Prosthesis use in persons with lower- and upper-limb amputation," *J. Rehabil. Res. Dev.*, vol. 45, no. 7, pp. 961–972, 2008.

[5] C. Gosselin, F. Pelletier, and T. Laliberte, "An anthropomorphic underactuated robotic hand with 15 dofs and a single actuator," in *2008 IEEE International Conference on Robotics and Automation*, 2008, pp. 749–754.

[6] S. Tanrıkulu, Ş. Bekmez, A. Üzümcügil, and G. Leblebicioğlu, "Anatomy and Biomechanics of the Wrist and Hand," in *Sports Injuries: Prevention, Diagnosis, Treatment and Rehabilitation*, M. N. Doral and J. Karlsson, Eds. Berlin, Heidelberg: Springer Berlin Heidelberg, 2015, pp. 441–447.

[7] C. Pylatiuk, S. Schulz, and L. Döderlein, "Results of an Internet survey of myoelectric prosthetic hand users," *Prosthet. Orthot. Int.*, vol. 31, pp. 362–70, Jan. 2008.

[8] J. Koprnický, P. Najman, and J. Šafka, "3D printed bionic prosthetic hands," *2017 IEEE Int. Workshop Electron. Control Meas. Signals Their Appl. Mechatron. ECMSM*, pp. 1–6, 2017.

[9] "Sri Lanka School of Prosthetics and Orthotics (SLSPO) - International Society for Prosthetics and Orthotics." [Online]. Available: https://www.ispoint.org/page/Edu_SriLanka_SLSPO. [Accessed: 26-Aug-2019].

[10] N. Wiener, *Cybernetics Or Control and Communication in the Animal and the Machine*. MIT Press, 1965.

[11] R. Meier and D. Atkins, "Functional Restoration of Adults and Children with Upper Extremity Amputation," *Res Trends Twenty-First Century*, vol. 30, no. 30, pp. 353–360, 2004.

[12] R. J. Schwarz and C. L. Taylor, "The anatomy and mechanics of the human hand," *Artif. Limbs*, vol. 2, no. 2, pp. 22–35, 1955.

[13] P. K. Levangie and C. C. Norkin, "Joint Structure and function: a comprehensive analysis. 3rd," *Phila. FA Davis Co.*, 2000.

[14] A. Freivalds, *Biomechanics of the upper limbs: mechanics, modeling and musculoskeletal injuries*. CRC press, 2011.

[15] M. Batmanabane and S. Malathi, “Movements at the carpometacarpal and metacarpophalangeal joints of the hand and their effect on the dimensions of the articular ends of the metacarpal bones,” *Anat. Rec.*, vol. 213, no. 1, pp. 102–110, 1985.

[16] A. Steindler, *Kinesiology of the human body under normal and pathological conditions*. Thomas Springfield, 1955.

[17] Y. Youm, R. Y. McMURTHY, A. E. Flatt, and T. E. Gillespie, “Kinematics of the wrist. I. An experimental study of radial-ulnar deviation and flexion-extension.,” *J. Bone Joint Surg. Am.*, vol. 60, no. 4, pp. 423–431, 1978.

[18] “Muscles,” *Pinterest*. [Online]. Available: https://www.pinterest.com/jessicaliles/muscles/. [Accessed: 27-Aug-2019].

[19] M. Herath, R. Gopura, and T. Lalitharatne, “An Underactuated Linkage Finger Mechanism for Hand Prostheses,” *Mod. Mech. Eng.*, vol. 08, pp. 121–139, Jan. 2018, doi: 10.4236/mme.2018.82009.

[20] C. Medynski and B. Rattray, “Bebionic prosthetic design,” in *Myoelectric Symposium*, 2011.

[21] S. C. Jacobsen, J. E. Wood, D. F. Knutti, and K. B. Biggers, “The UTAH/MIT dextrous hand: Work in progress,” *Int. J. Robot. Res.*, vol. 3, no. 4, pp. 21–50, 1984.

[22] J. K. Salisbury and J. J. Craig, “Articulated hands: Force control and kinematic issues,” *Int. J. Robot. Res.*, vol. 1, no. 1, pp. 4–17, 1982.

[23] G. A. Bekey, R. Tomovic, and I. Zeljkovic, “Control architecture for the Belgrade/USC hand,” in *Dextrous robot hands*, Springer, 1990, pp. 136–149.

[24] J. Butterfa\s s, M. Grebenstein, H. Liu, and G. Hirzinger, “DLR-Hand II: Next generation of a dextrous robot hand,” in *Proceedings 2001 ICRA. IEEE International Conference on Robotics and Automation (Cat. No. 01CH37164)*, 2001, vol. 1, pp. 109–114.

[25] “How the i-limb works | Touch Bionics.” [Online]. Available: http://www.touchbionics.com/products/how-i-limb-works. [Accessed: 27-Aug-2019].

[26] “VINCENTevolution 2.” [Online]. Available: https://vincentsystems.de/en/prosthetics/vincent-evolution-2/. [Accessed: 27-Aug-2019].

[27] D. G. K. Madusanka, L. N. S. Wijayasingha, R. Gopura, Y. W. R. Amarasinghe, and G. K. I. Mann, “A review on hybrid myoelectric control systems for upper limb prosthesis,” in *2015 Moratuwa Engineering Research Conference (MERCon)*, 2015, pp. 136–141.

[28] J. L. Pons *et al.*, “The MANUS-HAND dextrous robotics upper limb prosthesis: mechanical and manipulation aspects,” *Auton. Robots*, vol. 16, no. 2, pp. 143–163, 2004.

[29] M. Johnsson and C. Balkenius, “LUCS haptic hand III-An anthropomorphic robot hand with proprioception,” *LUCS Minor*, vol. 13, no. 2007, 2007.

[30] “DLR - Institute of Robotics and Mechatronics - Data sheet of DLR Hand II.” [Online]. Available: https://www.dlr.de/rm-neu/en/desktopdefault.aspx/tabid-3802/6102_read-8922/. [Accessed: 27-Aug-2019].

[31] I. Yamano and T. Maeno, “Five-fingered robot hand using ultrasonic motors and elastic elements,” in *Proceedings of the 2005 IEEE International Conference on Robotics and Automation*, 2005, pp. 2673–2678.

[32] I. N. Gaiser, C. Pylatiuk, S. Schulz, A. Kargov, R. Oberle, and T. Werner, “The FLUIDHAND III: A multifunctional prosthetic hand,” *JPO J. Prosthet. Orthot.*, vol. 21, no. 2, pp. 91–96, 2009.

[33] S. A. Dalley, D. A. Bennett, and M. Goldfarb, “Functional assessment of the vanderbilt multigrasp myoelectric hand: A continuing case study,” in *2014 36th Annual International Conference of the IEEE Engineering in Medicine and Biology Society*, 2014, pp. 6195–6198.

[34] C. Cipriani, M. Controzzi, and M. C. Carrozza, “The SmartHand transradial prosthesis,” *J. Neuroengineering Rehabil.*, vol. 8, no. 1, p. 29, 2011.

[35] Y. Losier *et al.*, “An overview of the UNB hand system,” in *Proceeding of the 2011 Myoelectric Controls/Powered Prosthetics Symposium*, 2011.

[36] L. Resnik, S. L. Klinger, and K. Etter, “The DEKA Arm: Its features, functionality, and evolution during the Veterans Affairs Study to optimize the DEKA Arm,” *Prosthet. Orthot. Int.*, vol. 38, no. 6, pp. 492–504, 2014.

[37] A. Polhemus, B. Doherty, K. Mackiw, R. Patel, and M. Paliwal, “uGrip II: A novel functional hybrid prosthetic hand design,” in *2013 39th Annual Northeast Bioengineering Conference*, 2013, pp. 303–304.

[38] R. Gopura and S. Bandara, “A Hand Prosthesis with an Under-Actuated and Self-Adaptive Finger Mechanism,” *Engineering*, vol. 10, pp. 448–463, Jan. 2018, doi: 10.4236/eng.2018.107031.

Appendix A : Outline drawing

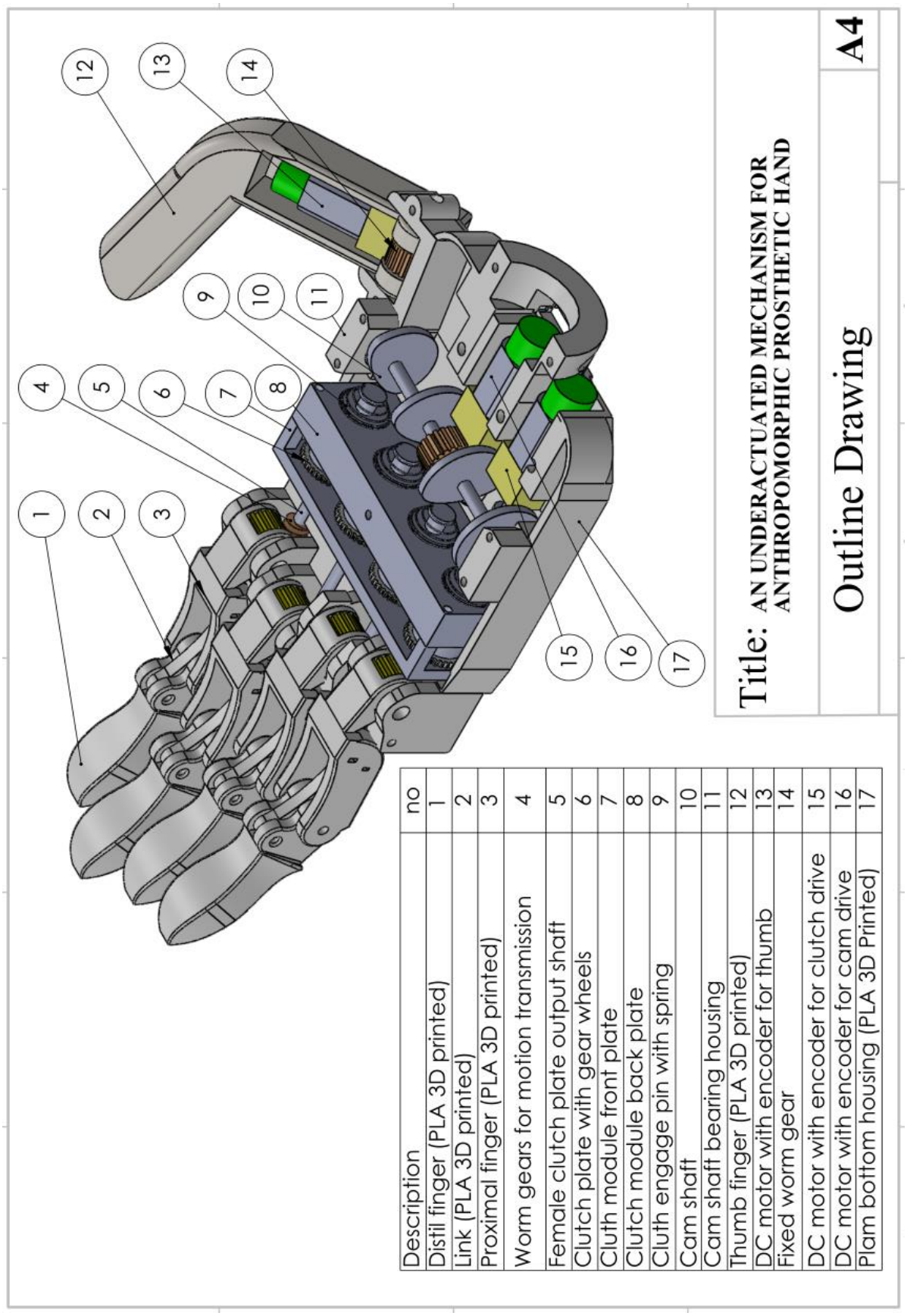

Description	no
Distil finger (PLA 3D printed)	1
Link (PLA 3D printed)	2
Proximal finger (PLA 3D printed)	3
Worm gears for motion transmission	4
Female clutch plate output shaft	5
Clutch plate with gear wheels	6
Cluth module front plate	7
Clutch module back plate	8
Cluth engage pin with spring	9
Cam shaft	10
Cam shaft bearing housing	11
Thumb finger (PLA 3D printed)	12
DC motor with encoder for thumb	13
Fixed worm gear	14
DC motor with encoder for clutch drive	15
DC motor with encoder for cam drive	16
Plam bottom housing (PLA 3D Printed)	17

Appendix B : Specifications of DC gear motor with encoder

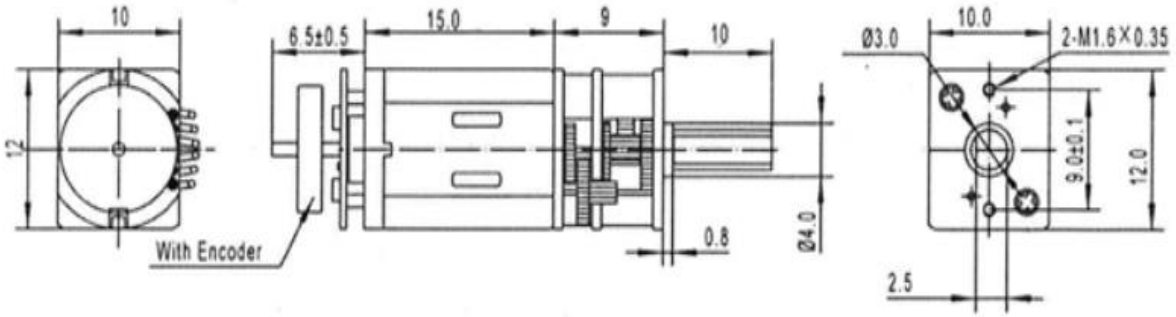

Parameter	Valve
Voltage (Nominal)	12 v
Voltage Range (Recommended)	6v – 12 v
Speed (No load)	90 rpm
Current (No load)	70 mA
Current Stall	1600 mA
Torque (Stall)	70 oz-in
Gear Ration	297.924 : 1
Encoder : Countable events per revolution (motor shaft)	12
Encoder : Countable events per revolution (Output shaft)	3,0575.0855
Encoder type	Relative, Quadrature
Encoder sensor type	Magnetic (Hall Effect)

Electrical characteristics of encoder

CHARACTERISTICS	SYMBOL	TEST CONDITIONS	MIN.	REF.	MAX.	UNITS
Input Voltage	Vcc	— — —	3.5	—	20	V
Output Saturation Voltage	Vce(sat)	Vcc=14V ;Ic=20mA	—	300	700	mV
Output Leakage Current	Icex	Vce=14V;Vcc=14V	—	<0.1	10	μV
Input Current	Ice	Vcc=20V; Output open	—	5	10	mA
Output Rise Time	t_r	Vcc=14V;R_L=820Ω;C_L=20pF	—	0.3	1.5	μS
Output Fall Time	t_f	Vcc=14V;R_L=820Ω;C_L=20pF	—	0.3	1.5	μS

Appendix C : Specifications of motor driver

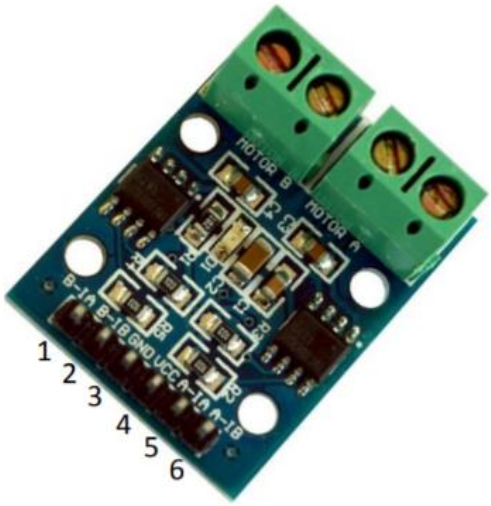

1	B-IA: Motor B Input A
2	B-IB: Motor B Input B
3	GND: ground
4	VCC: 2.5V-12V DC
5	A-IA: Motor A Input A
6	A-IB: Motor B Input B

Specifications

- On-board 2 L9110 motor control chip
- Module can be driven by two dc motors at the same time or one phase 4 line 2 type stepping motor
- Input voltage: 2.5-12V DC
- Each channel has a continuous output current 800 ma
- PCB Size: 29.2mm x 23mm

Schematic diagram

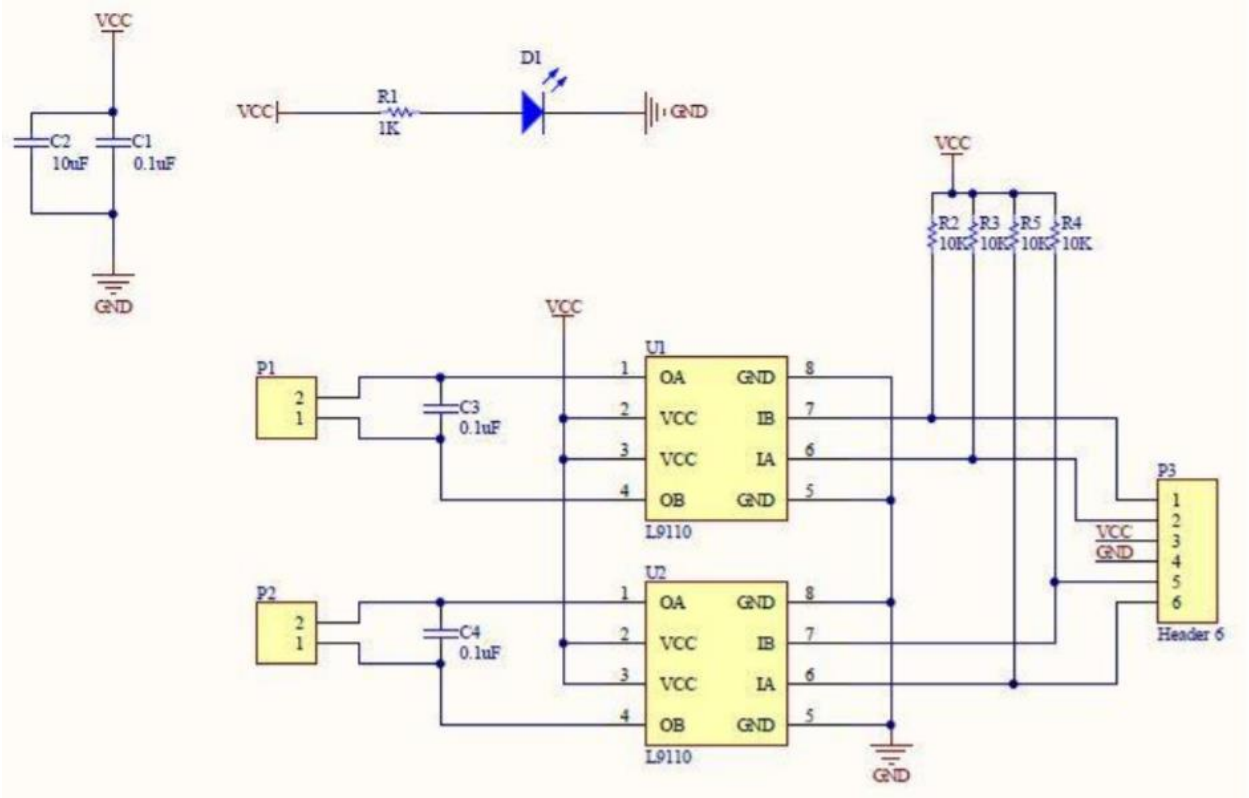

Appendix D : Arduino code

```
#include <Encoder.h>

Encoder EnDrive(2,3);   //Encoder for Drive
Encoder EnCam(18,19);    //Encoder for Cam positioning
Encoder EnThumb(20,21);  //Encoder for Thumb

//Arduino pin assigement for motor drivers
int Drive_A = 4;
int Drive_B = 5;
int Cam_A = 6;
int Cam_B = 7;
int Thumb_A = 8;
int Thumb_B = 9;

void setup() {

pinMode(Drive_A, OUTPUT);
pinMode(Drive_B, OUTPUT);

pinMode(Cam_A, OUTPUT);
pinMode(Cam_B, OUTPUT);

pinMode(Thumb_A, OUTPUT);
pinMode(Thumb_B, OUTPUT);

  Serial.begin(9600);

Serial.println("#1 :- MOTION - INDEX FINGER EXTENSION ");
Serial.println("#2 :- MOTION - INDEX FINGER FLEXION ");
```

```
Serial.println("#3 :- Drive manual For ");
Serial.println("#4 :- Drive manual Back ");
Serial.println("#5 :- Cam manual For ");
Serial.println("#6 :- Cam manual Back ");
Serial.println("#7 :- Thumb manual For ");
Serial.println("#8 :- Thumb manual Back ");
Serial.println("#9 :- EMERGENCY STOP ");

   while(!Serial);
  }
long oldPosition1  = -999;
long oldPosition2  = -999;
long oldPosition3  = -999;
void loop() {
if (Serial.available()){
int state = Serial.parseInt();

switch (state) {
  case 1:
Serial.println("#1 :- Flexion Series ACTIVATED ");
  while(EnCam.read() > -8500){    // encoder value found by experiements which stops finger at correct location

 analogWrite(Cam_A,0);
 analogWrite(Cam_B,255);
    driveForBack ();
      // Serial.println(EnCam.read());
  }
    analogWrite(Cam_A,0);
    analogWrite(Cam_B,0);
    analogWrite(Drive_A,0);
```

```
   analogWrite(Drive_B,0);

delay(1000);

while(EnDrive.read() > -24000 ){

  analogWrite(Drive_A,255);
  analogWrite(Drive_B,0);
  //Serial.println(EnDrive.read());
  }
  analogWrite(Drive_A,0);
  analogWrite(Drive_B,0);
while(EnThumb.read() > -18000){
   analogWrite(Thumb_A,0);
analogWrite(Thumb_B,255);
//  Serial.println(EnThumb.read());
  }
analogWrite(Thumb_A,0);
analogWrite(Thumb_B,0);
      break;
case 2:
Serial.println("#2 :- Extension Series ACTIVATED");
while(EnThumb.read() < 0){

analogWrite(Thumb_A,255);
analogWrite(Thumb_B,0);
  //  Serial.println(EnThumb.read());
  }
analogWrite(Thumb_A,0);
analogWrite(Thumb_B,0);
```

```
delay(500);
while(EnDrive.read() < 0){
    analogWrite(Drive_A,0);
  analogWrite(Drive_B,255);
  //Serial.println(EnDrive.read());
  }
  analogWrite(Drive_A,0);
  analogWrite(Drive_B,0);
delay(500);
 while(EnCam.read() < 0){
    analogWrite(Cam_A,255);
   analogWrite(Cam_B,0);
//  Serial.println(EnCam.read());
  }
    analogWrite(Cam_A,0);
    analogWrite(Cam_B,0);
 break;
case 3:
Serial.println("#3 :- Drive manual For ACTIVATED");
analogWrite(Drive_A,0);
analogWrite(Drive_B,150);
//Extension of fingers
break;
case 4:
Serial.println("#4 :- Drive manual Back ACTIVATED");
analogWrite(Drive_A,150);
analogWrite(Drive_B,0);
//Flexion of fingers
break;
case 5:
```

```
Serial.println("#5 :- Cam manual For ACTIVATED");
analogWrite(Cam_A,0);
analogWrite(Cam_B,150);
//Anticlockwise ; from side pinky perspective
break;
case 6:
Serial.println("#6 :- Cam manual Back ACTIVATED");
analogWrite(Cam_A,150);
analogWrite(Cam_B,0);
//Clockwise ; from side pinky perspective
break;
case 7:
Serial.println("#7 :- Thumb manual For ACTIVATED ");
analogWrite(Thumb_A,0);
analogWrite(Thumb_B,150);
//Thumb Flexion
break;
case 8:
Serial.println("#8 :- Thumb manual Back ACTIVATED");
analogWrite(Thumb_A,150);
analogWrite(Thumb_B,0);
//Thumb Extension
break;
case 9:
Serial.println("#9 :- EMERGENCY STOP ACTIVATED");
analogWrite(Drive_A,0);
analogWrite(Drive_B,0);
analogWrite(Cam_A,0);
analogWrite(Cam_B,0);
analogWrite(Thumb_A,0);
```

```
analogWrite(Thumb_B,0);
      break;
}
}
}
void driveForBack (){
  analogWrite(Drive_A,0);
  analogWrite(Drive_B,255);
  delay(500);
  analogWrite(Drive_A,225);
  analogWrite(Drive_B,0);
  delay(500);
  }
```

Appendix E : Matlab simulation code

```
clc;
clear all;

% Link Lengths
L1 = 9; %A = 9;
L2 = 36;%C = 36;
L3 = 37;%B = 37;
L4 = 10;%D = 10;

L5 = 43.45;
L6 = 34.79;

t= 0.8:0.05:2.5;
ang_speed = 1;
theta1 = ang_speed * t ;


%From Freudenstein Equation
K1 =  ((L4)^2 - (L2)^2 - (L3)^2 - (L1)^2 +
2*L2*L1.*cos(theta1)) / (2*L3) ;
K2 = (L1 - L2.*cos(theta1));
K3 = (-L2.*sin(theta1));

A = (K1+K2);
B = (-2*K3);
C = (K1-K2);

theta2 = 2 * atan ( (-(B) - sqrt((B).^2 - 4.*A.*C ))./(2.*A) )
;


P1 = [0;0];
P2 = [L1;0];

P3 = [L2.*cos(theta1); L2.*sin(theta1)];
P4 = [L1+L3.*cos(theta2); L3.*sin(theta2)];


% P5 point calculation

F = sqrt(L1^2 + L3^2 -2*L1*L3.*cos(pi-theta2));
mew = acos ( (F.^2+L4^2-L2^2) ./ (2.*F*L4) );

beta = (mew+0.45);
G = sqrt(L5^2 + F.^2 - 2*L5.*F.*cos(beta));
psi = acos((L2^2 + G.^2 - L6^2)./ (2*L2.*G));

omega = theta1- psi;
```

```
P5 = [G.*cos(omega);G.*sin(omega)];

for i=1:length (t)

 ani1 = subplot(1,1,1);

 hold on;
 P1_circle = viscircles(P1',0.05);
 P2_circle = viscircles(P2',0.05);
 P3_circle = viscircles(P3(:,i)',0.5);
 P4_circle = viscircles(P4(:,i)',0.05);
 P5_circle = viscircles(P5(:,i)',0.5);


    L1_line = line ([P1(1) P2(1)],[P1(2) P2(2)]);
    L2_line = line ([P1(1) P3(1,i)],[P1(2) P3(2,i)]);
    L3_line = line ([P2(1) P4(1,i)],[P2(2) P4(2,i)]);
    L4_line = line ([P3(1,i) P4(1,i)],[P3(2,i) P4(2,i)]);

    L5_line = line ([P3(1,i) P5(1,i)],[P3(2,i) P5(2,i)]);
    L6_line = line ([P4(1,i) P5(1,i)],[P4(2,i) P5(2,i)]);


title('Finger Trajectory');
xlabel('X (mm)');
ylabel('Y (mm)');

   axis(ani1,'equal');
   grid on;
   set(gca,'XLim',[-60 60],'YLim',[-5 80]);
hold off;

          pause(0.1);

  if i<length(t)

       delete( P1_circle);
       delete( P2_circle);
      % delete( P3_circle);
       %delete( P4_circle);
      % delete( P5_circle);
       delete( L1_line);
       delete( L2_line);
       delete( L3_line);
       delete( L4_line);
       delete( L5_line);
       delete( L6_line);


   end
end
```